

Palynological evidence reveals an arid early Holocene for the northeast Tibetan Plateau

Nannan Wang^{1,2}, Lina Liu^{1,2}, Xiaohuan Hou¹, Yanrong Zhang¹, Haicheng Wei³, and Xianyong Cao¹

¹Alpine Paleoeecology and Human Adaptation Group (ALPHA), State Key Laboratory of Tibetan Plateau Earth System, Environment and Resources (TPESER), Institute of Tibetan Plateau Research (ITPCAS), Chinese Academy of Sciences (CAS), Beijing 100101, China

²University of the Chinese Academy of Sciences, Beijing 100049, China

³Qinghai Provincial Key Laboratory of Geology and Environment of Salt Lakes, Xining 810008, China

Correspondence: Xianyong Cao (xcao@itpcas.ac.cn)

Received: 21 May 2022 – Discussion started: 13 June 2022

Revised: 1 September 2022 – Accepted: 13 September 2022 – Published:

Abstract. Situated within the triangle of the East Asian monsoon, the Indian monsoon, and the westerlies, the Holocene patterns of climate and vegetation changes on the northeast Tibetan Plateau are still unclear or even contradictory. By investigating the distribution of modern pollen taxa on the east Tibetan Plateau, we infer the past vegetation and climate since 14.2 ka BP (1000 years before present) from a fossil pollen record extracted from Gahai Lake (102.3133° E, 34.2398° N; 3444 m a.s.l.) together with multiple proxies (grain size, contents of total organic carbon and total nitrogen) on the northeast Tibetan Plateau. Results indicate that the Gahai Basin was covered by arid alpine steppe or even desert between 14.2 and 7.4 ka BP with dry climatic conditions, and high percentages of arboreal pollen are thought to be long-distance wind-transported grains. Montane forest (dominated by *Abies*, *Picea*, and *Pinus*) migrated into the Gahai Basin between 7.4 and 3.8 ka BP driven by wet and warm climatic conditions (the climate optimum within the Holocene) but reverted to alpine steppe between 3.8 and 2.3 ka BP, indicating a drying climate trend. After 2.3 ka BP, vegetation shifted to alpine meadow represented by increasing abundances of Cyperaceae, which may reflect a cooling climate. The strange pollen spectra with high abundances of Cyperaceae and high total pollen concentrations after ca. 0.24 ka BP (1710 CE) could be an indication of disturbance by human activities to some extent, but needs more direct evidence to be confirmed. Our study confirms the occurrence of a climate optimum in the mid-Holocene on the northeast Tibetan Plateau, which is consistent with climate records from

the fringe areas of the East Asian summer monsoon, and provides new insights into the fluctuations in the intensity and extent of the Asian monsoon system.

1 Introduction

Vegetation, as an essential component in the terrestrial ecosystem, responds to and is a good representation of environmental and climatic changes. Investigating the patterns and mechanisms of past vegetation changes provides a reliable analogue for predicting future climate and vegetation changes (Mykleby et al., 2017; Zhao et al., 2017). Since the sharp climate warming during the last deglaciation (after ca. 15 ka BP in the Northern Hemisphere; Wang et al., 2001; Andersen et al., 2004; Dykoski et al., 2005; Xu et al., 2013), the response of vegetation to climate warming could be a valuable palaeo-analogue for understanding current vegetation changes under global warming and for predicting future vegetation trends (Birks, 2019).

The northeast Tibetan Plateau lies in the transition between the East Asian summer monsoon, the Indian summer monsoon, and the westerlies, is sensitive to climate change, and is an ideal region to study past vegetation and climate variation (Bryson, 1986; An et al., 2012; Chen et al., 2016). Nevertheless, the climate records from different lacustrine sediments on the northeast Tibetan Plateau show a lack of consistency, for example, regarding the climatic conditions during the early Holocene. Some records reveal that the cli-

mate was relatively dry on the northeast Tibetan Plateau and controlled by the East Asian monsoon during the early Holocene (Shen et al., 2005; Herzschuh et al., 2006; Cheng et al., 2013), while other records such as those from Hala Lake and Genggahai Lake show that there was maximum water depth and hence a climatic optimum in the early Holocene (Qiang et al., 2013; Yan and Wünnemann, 2014; Wang et al., 2021). Therefore, more studies are needed to clarify the early Holocene climatic conditions, which are necessary to resolve the environmental evolution of the northeast Tibetan Plateau.

Pollen plays an important role in reconstructing the past vegetation and climate owing to its preservation in various sediment types (Chevalier et al., 2020). However, pollen-based vegetation and climate reconstructions on the Tibetan Plateau are also confronted with challenges for instance, the current quantitative reconstructions of vegetation and climate are based on pollen percentages, which can be biased when there is much exogenous arboreal pollen, especially in strata with extremely low pollen concentrations because the exogenous arboreal pollen will form a larger proportion of the pollen sample (Herzschuh, 2007; Ma et al., 2017, 2019). Exogenous arboreal pollen can be recognized in areas far away from forested regions, mainly because no trees grow around the lake or its adjacent areas nowadays, such as Luanhaizi Lake (Herzschuh et al., 2010), Donggi Cona Lake (Wang et al., 2014), and Kuhai Lake (Wischniewski et al., 2011). Arboreal pollen can then be excluded in subsequent analysis to ensure the correct interpretation of vegetation and environment. However, it is somewhat difficult to recognize the contribution of exogenous pollen from areas near the forest on the eastern part of the Tibetan Plateau, which could seriously impact the results of vegetation reconstructions, such as from Naleng Lake (Kramer et al., 2010) and Qinghai Lake (Shen et al., 2005). Solving this issue of clarifying the influence of exogenous pollen is an important prerequisite for a better understanding of the early Holocene climate shifts. Understanding the spatial distribution characteristics of modern pollen and their relationships may be an effective way to identify such arboreal pollen properties.

In this study, we integrate multiproxy records, e.g. pollen, grain size, total organic carbon (TOC) and total nitrogen (TN) of Gahai Lake to reconstruct the climate and vegetation evolution since the last deglaciation. We assess the dispersal ability and biotopes of the main pollen taxa in the pollen record by investigating the distribution of modern pollen and their relationship with the climate. We attempt to recognize exogenous pollen and evaluate the influence on reconstruction results to determine whether the early Holocene of the northeast Tibetan Plateau was dry or wet.

2 Study area

Gahai Lake (102.3133° E, 34.2398° N; 3444 m a.s.l.) is situated in the upper reaches of the Yellow River on the northeast Tibetan Plateau, a transitional zone between the Tibetan Plateau, the mountainous area of Longnan, and the Loess Plateau (Fig. 1). Gahai Lake is a typical plateau interior freshwater lake, with a total area of 15 km² and a mean water depth ranging from 2 to 2.5 m. The water supply of the lake is mainly from precipitation, groundwater recharge, and surface runoff from surrounding mountains to the south and south-east including Qiongmuequ, Wenniqu, and Geqionkuhe rivers, and there is a single outflow stream at the north-western end of the basin (Duan et al., 2016; Fig. 1). Gahai Lake currently belongs to the alpine humid climate zone, which is influenced by the West Pacific Subtropical High in summer and controlled by westerlies in winter. Climate characteristics are rain in the warm season, and large seasonal and diurnal temperature differences (Liang, 2006). Mean annual temperature of this region is 1.2 °C and mean annual precipitation is 782 mm, with about 80 % of precipitation falling in the rainy season (from June to September), and mean annual evaporation is 1150 mm (Duan et al., 2016).

Vegetation cover in the Gahai Basin exceeds 90 %. There are abundant species in the grassland community, which is at the intersection of various flora, and perennial herbs predominate. The dominant plant species include *Poa annua*, *Carex*, *Clintoniaudensis*, *Polygonum*, *Ranunculus japonicus*, *Potentilla fruticosa*, *Neyraudia reynaudiana*, and *Elymus nutans*. Forest is found in the eastern low mountains with a mosaic distribution of meadow and shrub, dominated by *Abies*, *Picea*, *Betula*, and Cupressaceae. *Picea* is found in damp areas at the foot of mountains and replaced by *Betula* as a transitional community after being cut down; *Abies* occurs on shady and semi-shady slopes between 3200 and 3400 m a.s.l.; Cupressaceae is distributed mostly on sunny and semi-sunny slopes of more than 35°. This region belongs to a typical stockbreeding district, and the grazing activity focuses on the grassland. In addition, there is small-scale agriculture along the river valley at low elevations (Liang et al., 2006; Duan et al., 2016).

3 Material and methods

3.1 Modern pollen data and their climate data

Our modern pollen dataset ($n = 731$) is derived from the east Tibetan Plateau ranging from 94.07 to 103.02° E and from 29.13 to 38.48° N, with elevations from 2515 to 5008 m a.s.l. These modern pollen data are mainly from the modern pollen database of China and Mongolia (Cao et al., 2014) and recently published pollen data for the east Tibetan Plateau (Cao et al., 2021; Wang et al., 2022). The pollen sites are generally evenly distributed across the east Tibetan Plateau, covering subalpine forest, alpine meadow, alpine steppe, and alpine

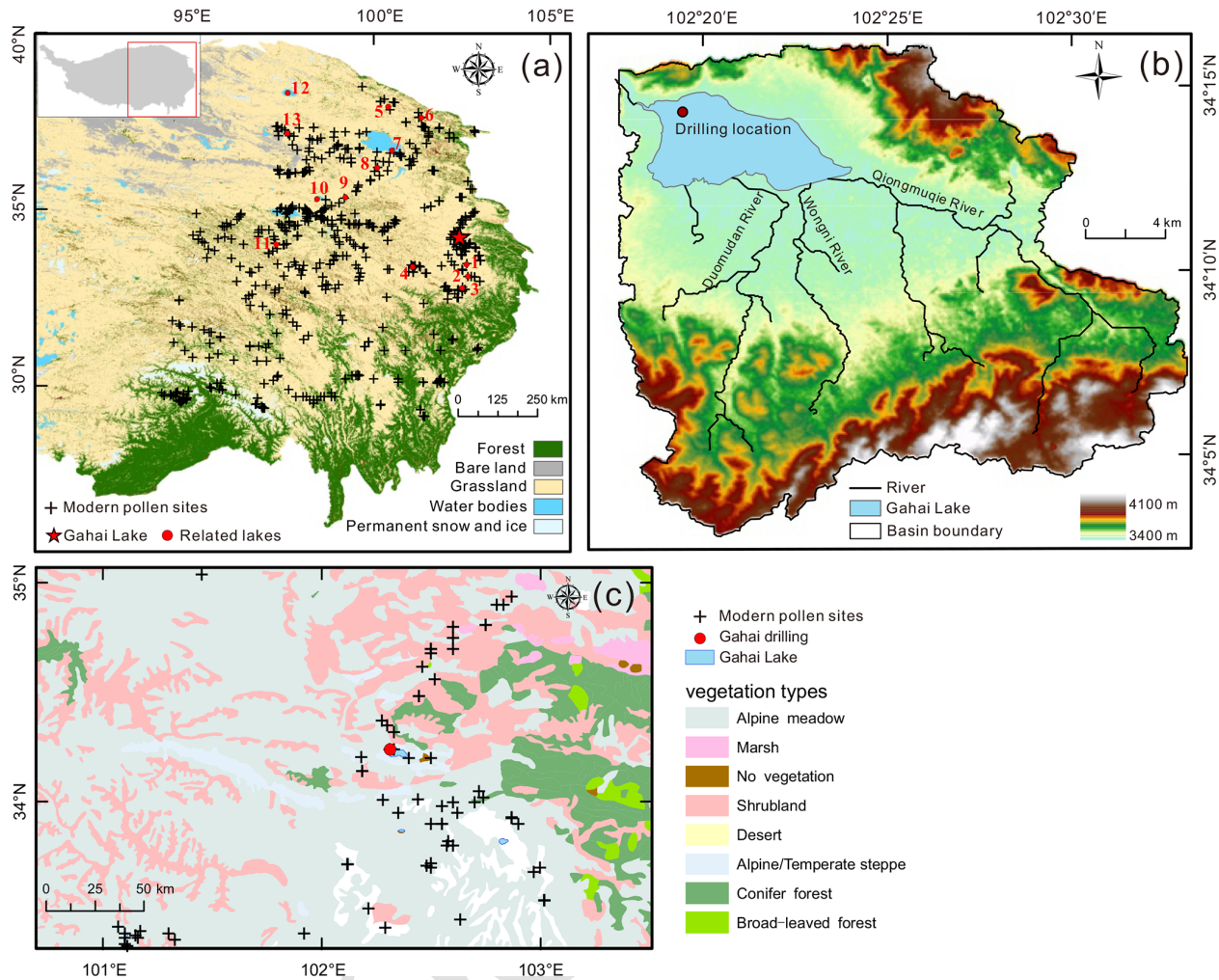


Figure 1. (a) The locations of the related lakes and modern surface samples (Du, 2019). Lakes referred to in the text: 1, ZB08-C1; 2, ZB10-C14; 3, Hongyuan peatland; 4, Ximencuo Lake; 5, Dalianhai Lake; 6, Luanhaizi Lake; 7, Qinghai Lake; 8, Genggahai Lake; 9, Kuhai Lake; 10, Donggi Cona Lake; 11, Koucha Lake; 12, Hala Lake; 13, Gahai Lake (Qaidam basin). (b) Catchment map and coring site of Gahai Lake. (c) Distribution of modern pollen samples in the vicinity of Gahai Lake.

desert (Fig. 1). Pollen sample types include topsoil, lake surface sediments, and moss polsters mainly.

We selected four important climate variables including mean annual precipitation (P_{ann}), mean temperature of the warmest month (Mt_{wa}), mean temperature of the coldest month (Mt_{co}), and mean annual temperature (T_{ann}), together with elevation (Elev) to investigate the relationship between pollen assemblages and the environment because these are important factors influencing the pollen distribution on the Tibetan Plateau (Lu et al., 2011; Cao et al., 2021; Wang et al., 2022). Modern climatic data were obtained from the Chinese Meteorological Forcing Dataset (CMFD; gridded near-surface meteorological dataset), and each sample is assigned to the nearest pixel of the CMFD using the *fields* package version 12.3 (Nychka et al., 2021) of R (version 4.0.3; R Core Team, 2021). The detailed processes of obtaining climatic data are presented in Fig. A1 (in the appendix).

3.2 Sediment sampling and radiocarbon dating

A 329 cm long sediment core (named GAH) was obtained using a UWITEC platform from the deepest part of Gahai Lake (ca. 2 m) in January 2019 (Fig. 1), and then transported to the Institute of the Tibetan Plateau Research for preservation. GAH was sub-sampled at 1 cm intervals, and all sub-samples were freeze-dried.

The age-depth model for GAH was established by ^{210}Pb , ^{137}Cs , and accelerator mass spectrometry (AMS) radiocarbon dating. The top 20 cm of the sediment was measured at 1 cm intervals for ^{210}Pb and ^{137}Cs at the School of Geographical Science, Nantong University. The constant rate of supply (CRS) model was selected to calculate the ^{210}Pb dates and the results revealed that the ^{210}Pb date of 1963 CE was mainly consistent with the ^{137}Cs peak (1963 CE), indicating this model was suitable and obtained a good effect (Appleby,

2001). Finally, an age-depth model based on a ^{210}Pb -CRS model corrected by the ^{137}Cs peak was generated (Fig. 4a). Overall, 13 bulk organic sediment samples of 1 cm thickness were sent for AMS ^{14}C dating by Beta Analytic Inc., USA, owing to a lack of macrofossils (Table 2). The age-depth model was established using the Bayesian age-depth modeling in the *rbacon* package (version 2.5.7; Blaauw and Christen 2011; Blaauw et al., 2021) in R (R Core Team, 2021) and the IntCal20 radiocarbon calibration curve (Reimer et al., 2020).

3.3 Laboratory analysis

The pollen samples (0.6–22 g; $n = 111$; at 1–2 cm intervals) were treated with hydrofluoric acid sieving analysis (Fægri and Iversen, 1989). *Lycopodium* spores (ca. 27 560 grains) were added to the samples to calculate the pollen concentration, then samples were processed with 10 % HCl, 10 % KOH, and 36 % HF, and sieved through a 7 μm nylon mesh, followed by acetolysis (9 : 1 mixture of acetic anhydride and sulfuric acid) treatment. Finally, glycerin was added to preserve the samples. The pollen taxa were identified and counted with a 400 \times LEICA DM 2500 optical microscope, with the aid of modern pollen reference slides collected from the eastern and central Tibetan Plateau (including 401 common species of alpine meadows; Cao et al., 2020) and published atlases for pollen and spores (Wang et al., 1995; Tang et al., 2017). At least 100 terrestrial pollen grains were counted for most samples, except for 10 samples owing to extremely low pollen concentration and more than 3000 *Lycopodium* spores were counted for each sample which could reflect the palaeo-vegetation at that time. Because of the low pollen concentrations below the depth of 176 cm, only pollen data for the upper part of the core are presented and discussed.

For the grain size analysis, freeze-dried samples (1 g; $n = 176$) were treated with 30 % H_2O_2 to remove organic matter and 10 % HCl to remove carbonate, cleaned with deionized water and kept stable for 24 h, before adding 0.5 N sodium hexametaphosphate (10 mL) and undergoing ultrasonic cleaning for 10 min. A laser diffraction particle size analyser MASTERSIZER 3000 (Chen et al., 2013) was used, with each sample being tested 3 times and their average value used in the final grain size data.

A total of 176 samples were analysed to obtain organic matter change since the last deglaciation, including TN and TOC. Catalysts were added to freeze-dried samples and reacted quickly. The TN was measured with an Elementar element analyser (CNS analyser, Vario MAX Cube), which has a measurement accuracy of 0.001. The TOC was measured with a Vario MAX C analyser, and has the same accuracy as TN. All samples were ground to ensure sufficient reaction before testing. The C/N ratio was calculated by dividing TOC by TN.

3.4 Numerical analyses

Ordination analyses were employed to investigate the modern relationship between pollen taxa and climatic variables for the eastern Tibetan Plateau. Pollen taxa (with $\geq 10\%$ maximum and ≥ 30 occurrences) from the 731 modern pollen assemblages were used for detrended correspondence analysis (DCA; Hill and Gauch, 1980). The length of the first axis of the pollen data was 3.29 SD (standard deviation units), indicating that a linear response model is suitable for the modern pollen dataset (ter Braak and Verdonschot, 1995). Hence, we performed redundancy analysis (RDA) to visualise the distribution of pollen species and sampling sites along the climatic gradients. We used the variance inflation factor (VIF) to determine high collinearities within the model, and stopped adding variables to ensure all VIF values are lower than 20 (ter Braak and Prentice, 1988; Table 1). All ordination analyses were run using the *rda* function in the *rioja* package version 0.9–26 (Juggins, 2020) in R, using square-root transformed modern pollen percentages to optimize the signal-to-noise ratio (Prentice, 1980).

For the fossil pollen dataset obtained from GAH, 22 pollen taxa (those present in at least 3 samples and with a $\geq 3\%$ maximum) with square-root transformed percentages were selected for ordination analyses. The length of the first axis was 1.67 SD, indicating that a principal component analysis (PCA) is suitable to investigate the relationship between the pollen taxa. The PCA was run using the *rda* function in the *vegan* package (version 2.5–4; Oksanen et al., 2019) in R.

In addition, weighted-averaging partial least squares (WA-PLS) was employed to establish a pollen-climate transfer function using the modern pollen dataset, and to quantitatively reconstruct past climate for the GAH pollen record. More details of the reconstruction are presented in the Supplement.

4 Results

4.1 Relationships of pollen taxa to climatic variables and elevation

The modern pollen dataset for the east Tibetan Plateau contains 107 pollen taxa and covers a long P_{ann} gradient (161–963 mm) and broad Mt_{wa} gradient (1.8–18.5 °C) (Figs. 2; A1). High abundances of arboreal pollen taxa including *Abies*, *Quercus* (evergreen, E), *Corylus*, and *Carpinus* are mainly distributed in regions with P_{ann} higher than 450 mm and Mt_{co} higher than $-15\text{ }^{\circ}\text{C}$ (Figs. 2; A1). *Pinus* (up to 2.3 %, mean 0.3 %), *Picea* (up to 25.7 %, mean 0.5 %), and *Betula* (up to 5.7 %, mean 0.4 %) are also widely distributed and appear in extremely dry and cold sampling sites where P_{ann} is lower than 450 mm and Mt_{co} lower than $-15\text{ }^{\circ}\text{C}$, although their high abundances are restricted to warm and wet areas (Figs. 2; A1). Drought-tolerant taxa such as *Chenopodiaceae* and *Ephedra* are restricted to regions with low P_{ann}

Table 1. Summary statistics for redundancy analysis (RDA) with 19 pollen taxa and 4 climate variables. VIF: variance inflation factor; P_{ann} : mean annual precipitation (mm); Mt_{co} : mean temperature of the coldest month ($^{\circ}\text{C}$); Mt_{wa} : mean temperature of the warmest month ($^{\circ}\text{C}$); T_{ann} : mean annual temperature ($^{\circ}\text{C}$); and Elev: elevation (m a.s.l.).

Climate variables	VIF (without T_{ann})	VIF (add T_{ann})	Climate variables as sole predictor	Marginal contribution based on climate variables	
			Explained variance (%)	Explained variance (%)	p -value
P_{ann}	3.0	3.1	5.2	7.1	0.001
Mt_{co}	4.5	133.6	4.9	0.3	0.001
Mt_{wa}	6.5	111.7	3.7	5.7	0.001
Elev	2.5	3.0	4.5	0.2	0.001
T_{ann}	–	403.9	–	–	–

and high Mt_{wa} , and they have quite low abundances in wet areas (Fig. 2). In addition, elevation is also an important factor influencing the pollen distribution on the eastern Tibetan Plateau. Arboreal pollen taxa including *Pinus*, *Picea*, *Abies*, *Betula*, *Quercus* (deciduous, D), and *Corylus* are mainly distributed in areas below 3900 m a.s.l., while *Quercus* (E) is concentrated in areas above 3700 m a.s.l. The high percentages of Cyperaceae, *Artemisia*, and *Chenopodiaceae* are mainly concentrated in the lower elevations (below 3200 m a.s.l.).

Redundancy analysis shows that the first two axes explain 28 % of the pollen data (axis 1: 15.5 %; axis 2: 12.5 %; Fig. 3). Arboreal pollen taxa are located in the left of the biplot and are positively correlated with P_{ann} and Mt_{co} . Asteraceae, Poaceae, *Thalictrum*, Ranunculaceae, Caryophyllaceae, and Cyperaceae show a negative relationship with Mt_{wa} and Mt_{co} while positive with Elev and are situated in the lower right of the biplot. Drought-tolerant pollen including *Chenopodiaceae*, *Artemisia*, and *Ephedra* are situated at the upper right of the biplot, showing positive correlations with temperature variables and negative correlations with precipitation (Fig. 3).

4.2 Sedimentary lithology and chronology

The sedimentary lithology of the GAH core is comprised of black silt in the upper part (0–99 cm), brown clay in the central part (99–240 cm), and dark-brown fine silt in the lower part (240–329 cm; Fig. 4). Our study concentrates on the vegetation and environment evolution of the upper 176 cm due to the extremely low pollen concentrations in the lower part, which are insufficient for statistical analyses.

The chronology of the upper 20 cm sediment is established by the ^{210}Pb -CRS model, with dates falling between 1828 and 2013 CE. The AMS ^{14}C ages of GAH exhibit a linear regression with depth, while there is a transient inversion between 191 and 279 cm, which is probably due to increased erosion input to the basin, leading to some old carbon accumulating in the lake. The ages of the upper 20 cm are calcu-

Table 2. AMS radiocarbon dates for Gahai Lake.

Lab ID	Depth (cm)	$\delta^{13}\text{C}$ (‰)	^{14}C age (years BP)	Error (\pm years)
Beta-546102	10	−25.6	440	30
Beta-546103	25	−25.1	1740	30
Beta-539751	40	−25.7	1960	30
Beta-539752	80	−24.8	3880	30
Beta-546104	99	−24.3	6390	30
Beta-539753	120	−22.1	8180	40
Beta-546105	144	−22.9	10 240	30
Beta-539754	170	−23	10 590	30
Beta-575823	191	−24.4	15 070	40
Beta-546120	229	−25.4	14 870	50
Beta-550230	275	−23.5	18 930	60
Beta-546121	279	−22.6	15 550	50
Beta-546122	319	−20.5	19 440	70

lated based on their relationship (Table 2), and the age difference between ^{14}C and ^{210}Pb of the same depth is considered as the reservoir age. We selected two depths (6 and 10 cm) to calculate an average to reduce errors and obtained a reservoir age of 483 years. The age-depth model suggests that the basal age of GAH is about 24 ka BP, with the age of sediments between 191 and 279 cm basically remaining the same, probably because of lake sediment collapse or rapid input of terrigenous clastic materials since the lithology also markedly changes between 190 and 280 cm, confirming that the lake underwent rapid deposition during this phase. The sedimentation rate has been relatively stable since 15 ka BP, and our research focuses on the vegetation and environmental evolution since 14.2 ka BP (Fig. 4).

4.3 Pollen record of GAH since the last deglaciation

In our study, 52 pollen taxa were identified in the 111 samples from the upper part of GAH (0–176 cm), with Cyperaceae, *Pinus*, Asteraceae, and *Artemisia* as dominant taxa, while Poaceae, Ranunculaceae, *Ulmus*, and *Picea* are com-

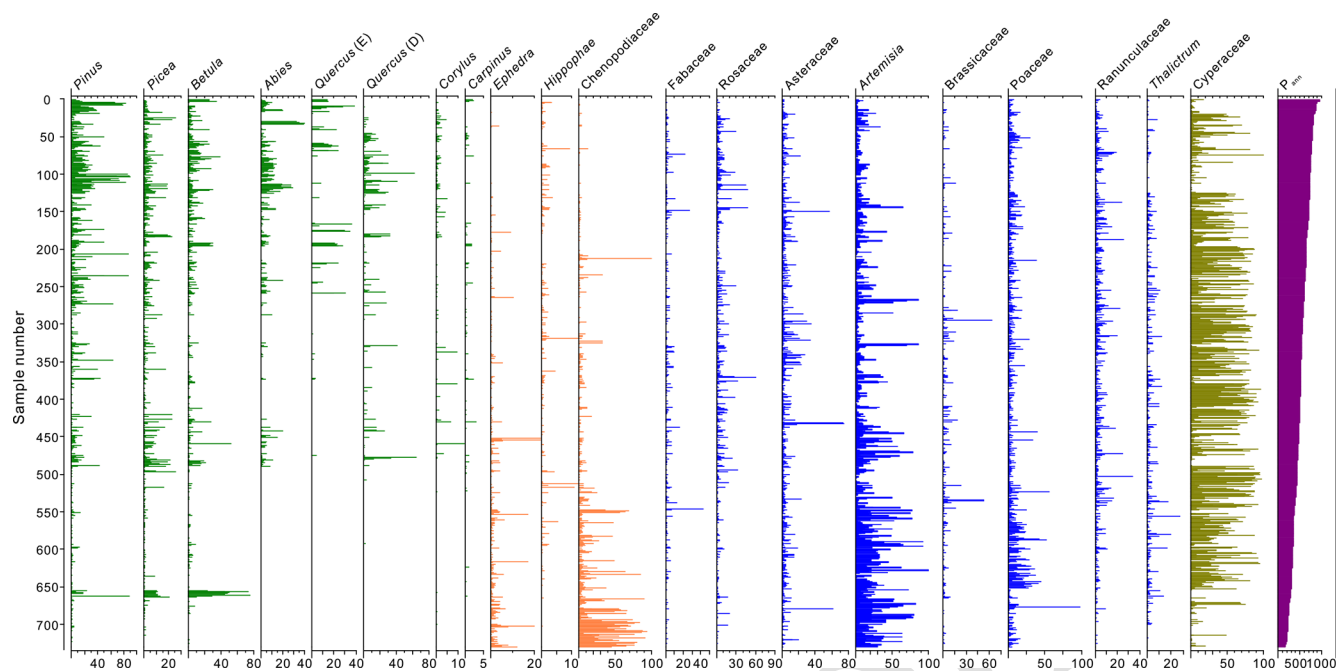


Figure 2. Pollen assemblages of surface sediment samples with annual precipitation (P_{ann}) from the eastern Tibetan Plateau.

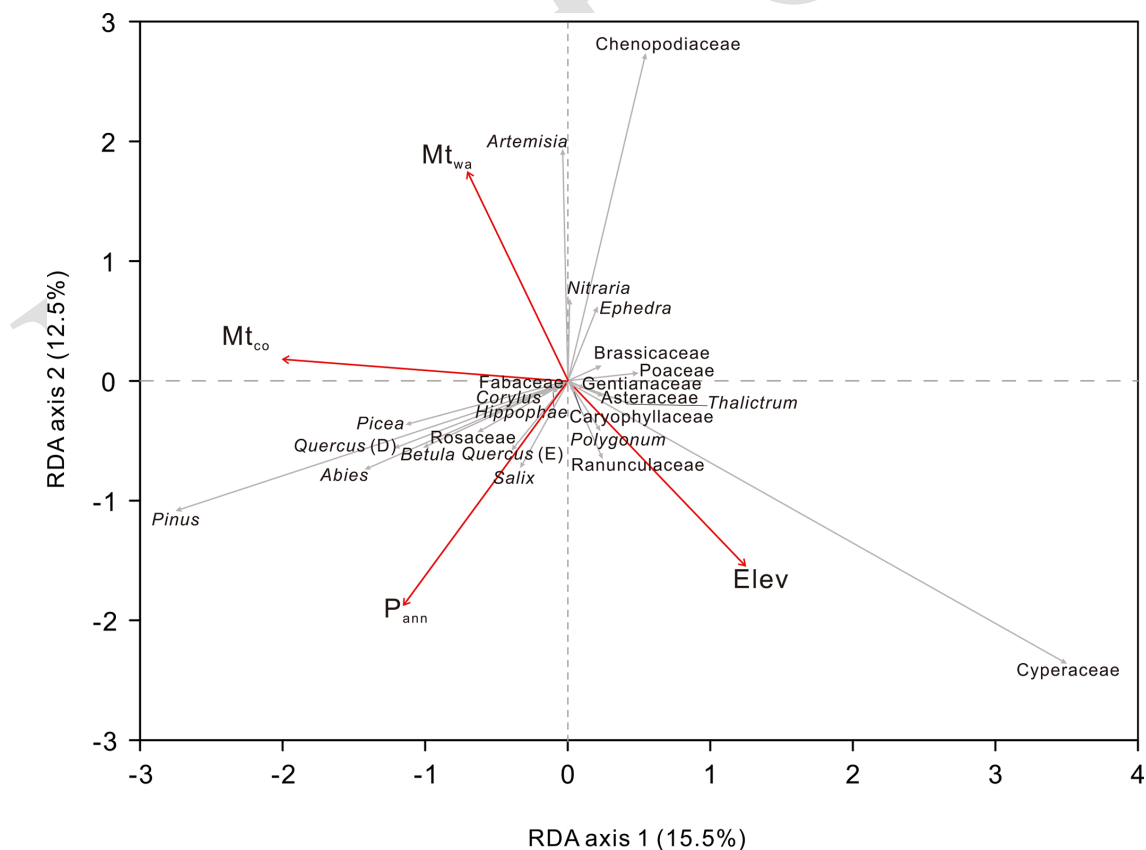


Figure 3. Redundancy analysis (RDA) of modern pollen samples along with three climate variables and elevation.

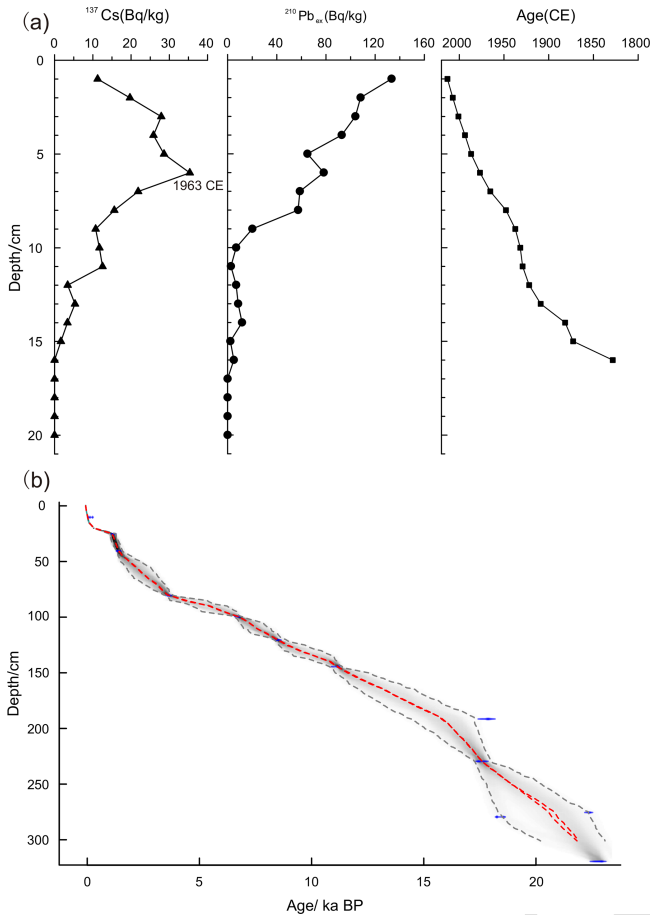


Figure 4. Age-depth model of the Gahai Lake sediment core derived from ^{137}Cs , ^{210}Pb , and ^{14}C dating. (a) Black line with triangles: ^{137}Cs age; black line with solid circles: ^{210}Pb : $^{210}\text{Pb}_{\text{ex}}$ age; black line with squares: mean age based on annual lamination counting. (b) Age-depth curve based on a ^{210}Pb profile of recent sediments and 13 AMS radiocarbon dates from Gahai Lake. The range of the two dashed grey lines indicates the 95 % confidence intervals, and the dashed red lines show the single “best” model based on the weighted mean age for each depth.

mon taxa. The pollen record can be demarcated into four zones (Fig. 5). Pollen concentration is extremely low (mean 33.5 grains per g) before 7.4 ka BP, and the pollen spectra are dominated by arboreal pollen taxa including *Pinus*, *Picea*, *Ulmus*, and *Betula*, together with abundant drought-tolerant pollen taxa (such as *Chenopodiaceae* and *Ephedra*). Pollen concentrations increase remarkably after 7.4 ka BP, and the percentage of drought-tolerant pollen taxa decreases while that of *Pinus* increases in the pollen spectra. Between 3.8 and 2.3 ka BP, *Pinus* and *Picea* decrease sharply, while *Artemisia*, *Poaceae*, *Asteraceae*, and *Thalictrum* increase significantly. Pollen concentrations increase greatly and the pollen spectra are dominated by *Cyperaceae* after 2.3 ka BP. *Cyperaceae* rises sharply and becomes overwhelmingly dominant in the

pollen spectra, and the pollen concentration also increases strongly in the last 0.24 ka BP (Fig. 5).

4.4 PCA results

The first two axes of the principal component analysis (PCA) explain 72 % of the total pollen data (axis 1: 59.2 %; axis 2: 12.8 %; Fig. 6a). The PCA divides arboreal pollen taxa (such as *Pinus*, *Picea*, *Betula*, *Ulmus*), alpine steppe taxa (including *Artemisia*, *Poaceae*, *Asteraceae*), and meadow taxa (*Cyperaceae*) into three clear groups. In addition, pollen samples of Zones I and II are consistent with arboreal taxa, pollen samples from Zone III contain abundant steppe taxa, while samples in Zone IV are dominated by *Cyperaceae* (Fig. 6b).

4.5 Sedimentology and conventional geochemistry

The size fractions (volume, %) were classified as clay (< 4 μm), silt (fine: 4–16 μm ; medium: 16–32 μm ; coarse: 32–63 μm , combined into one category for the discussion), and sand (> 63 μm), and the specific details are shown in Fig. A2. The grain size parameters of GAH include mean grain size, which ranges from 17.5 to 60 μm . The combined silt fraction (4–63 μm) accounts for the maximum proportion (58–75 %; mean 66 %) in general (Fig. 7). The clay fraction (15–33 %; mean 23 %) forms the highest proportion during 14.2–10.8 ka BP, then decreases significantly and remains stable after 10.8 ka BP (Fig. 7). The silt fraction (57.6–74.7 %; mean 63.9 %) is lowest during 14.2–10.8 ka BP, then increases and reaches a peak during 7.4–3.8 ka BP, after which the mean value decreases to 65.8 % (Fig. 7). The sand fraction correlates with the silt fraction before 10.8 ka BP, while later the variation is anticorrelated. Mean grain size closely correlates with the sand fraction in general (Fig. 7).

The TOC, TN, and C/N ratios fluctuate greatly after 14.2 ka BP, and TOC and TN present simultaneous change trends (Fig. 7). The TOC and TN values are remarkably low and C/N ratios are lower than 10 between 14.2 and 7 ka BP. TOC, TN, and C/N ratios increase significantly and C/N ratios are higher than 10 between 7 and 3.8 ka BP. TOC, TN, and C/N ratios reduce slightly but are still higher than 10 after 3.8 ka BP. The TOC and TN values increase drastically while C/N ratios have no obvious change during the last 0.24 ka BP (since 1710 CE).

5 Discussion

5.1 Patterns and interpretation of the proxies

The TOC is a proxy for the abundance of organic matter which originates from aquatic organisms and terrestrial vegetation, and TN represents the nutritional conditions of the lake. In addition, TOC is an effective index to evaluate the summer monsoon intensity, where low values reflect a cold and dry climate (An et al., 2012; Opitz et al., 2012). C/N

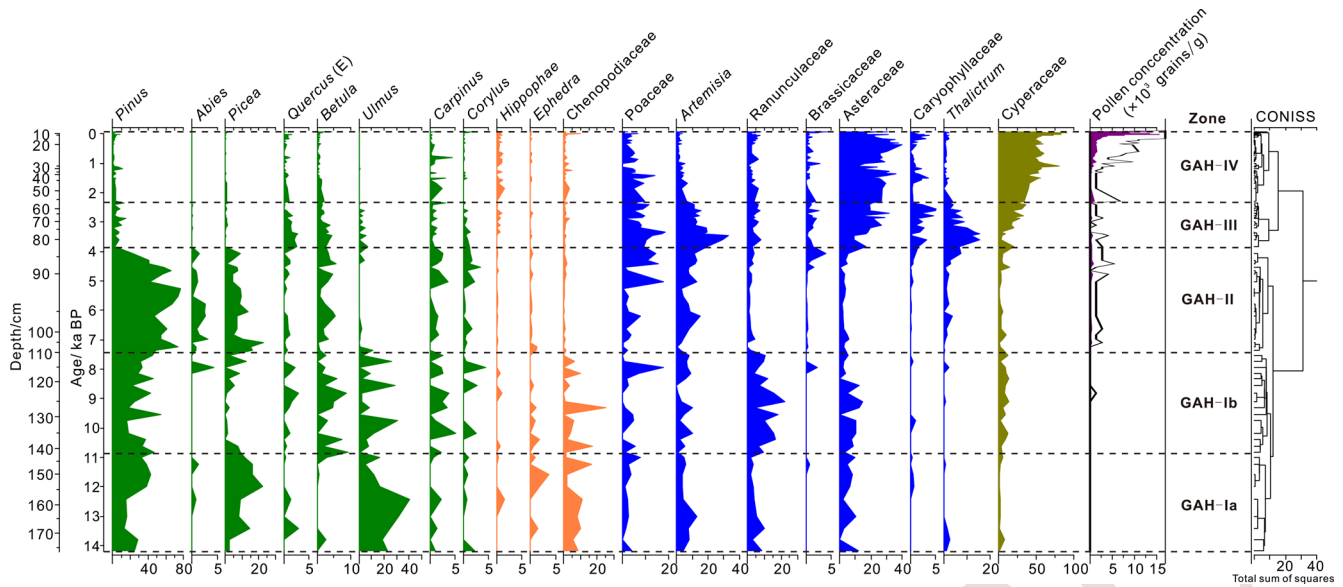


Figure 5. Pollen diagram of the main fossil pollen taxa in Gahai Lake, northeast Tibetan Plateau.

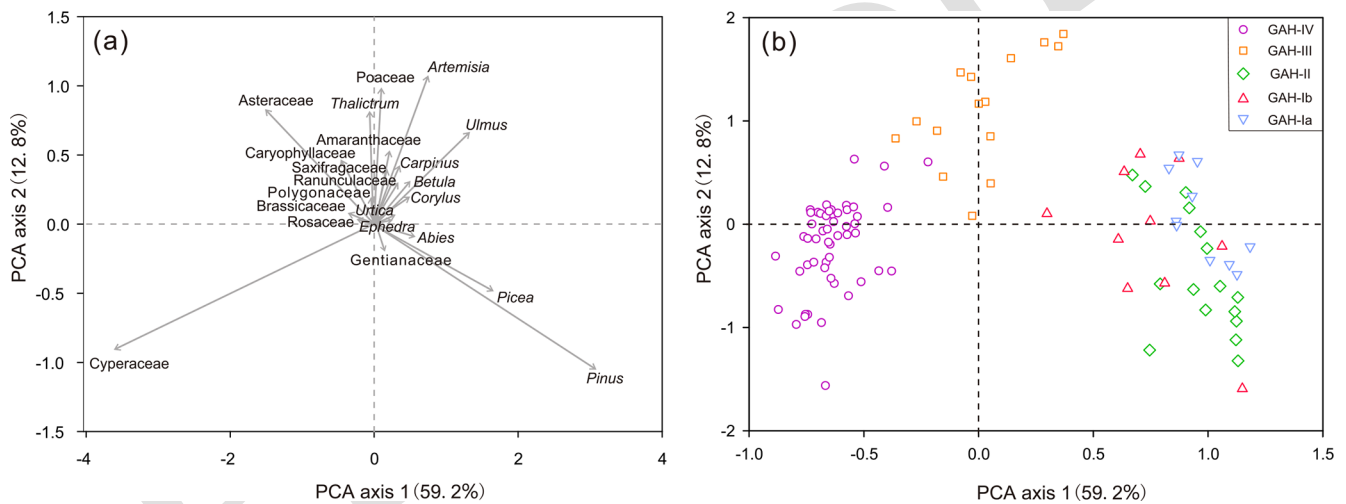


Figure 6. Principal component analysis (PCA) of fossil pollen taxa (a) and pollen zones (b) from Gahai Lake (see Fig. 5 for the pollen zones).

ratios are used to trace the plant source of the organic matter. C/N ratios of the nonvascular aquatic plants and algae are generally between 4 and 10, and C/N ratios > 20 indicate that organic matter mainly originates from terrestrial vascular plants. Ratios ranging from 10 to 20 suggest that the organic matter is derived from a mixture of aquatic and terrestrial plants (Meyers and Ishiwatari, 1993; Meyers, 2003; Kasper et al., 2015). High values of TOC and C/N ratios in the Tibetan Plateau lakes suggest a warm and wet climate (Chen et al., 2021).

The grain size composition of lake sediments can be used to trace the source of clastic particles, aeolian activity, and water level fluctuations, which reflect the regional climate

conditions (Håkanson and Jansson, 1983; Liu et al., 2016). The sources of lacustrine sediments include clastic materials carried by inflow rivers, aeolian inputs, and authigenic chemical deposition, and mean grain size reflects the intensity of transport dynamics (Folk and Ward, 1957; Xiao et al., 2013). There have been many particle size analyses from lacustrine sediments or loess deposits on the northeast Tibetan Plateau. For example, Qiang et al. (2014) analysed the grain size of Genggahai lake and propound that the sand fraction (> 63 μm) reflects aeolian activity. Chen et al. (2013) investigated Sugan Lake in the Qaidam Basin and argue that changes in the > 63 μm fraction reflect the frequencies of dust storms and strong winds. In addition, Wang et al. (2015)

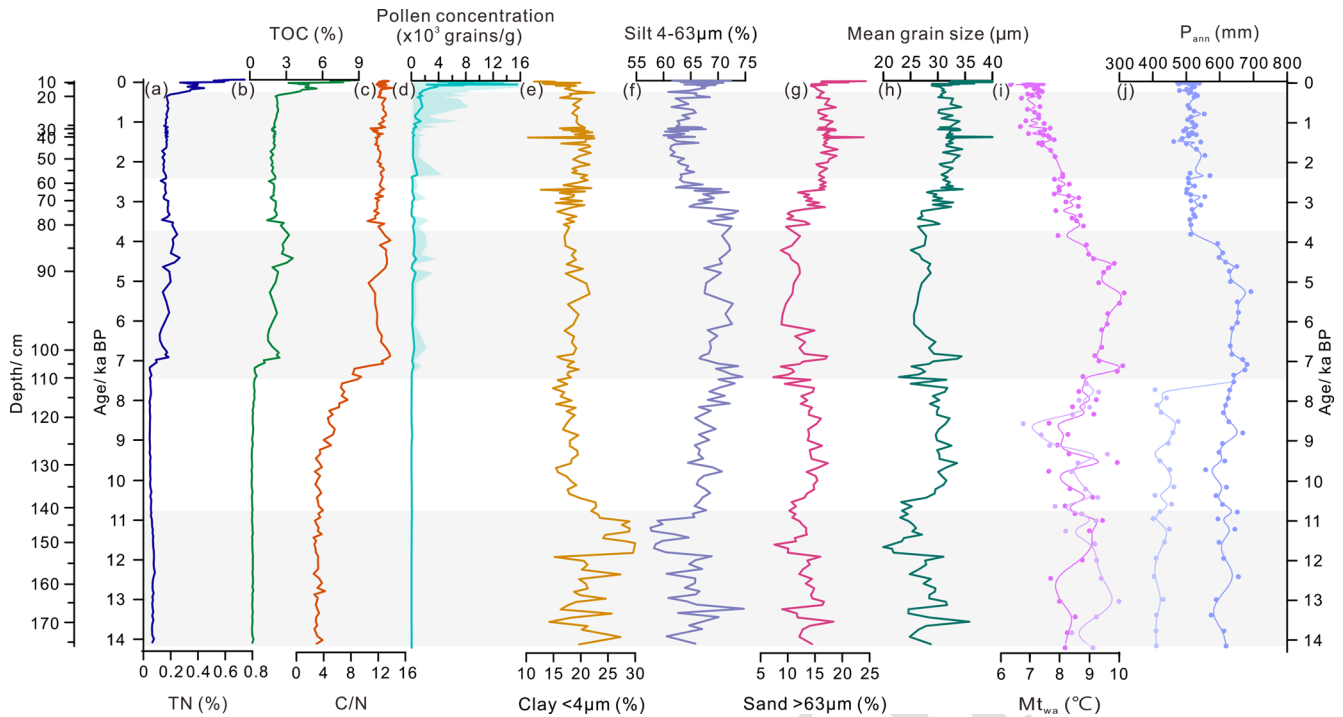


Figure 7. Comparison of the multiproxy records from Gahai Lake. (a) Total nitrogen (TN); (b) total organic carbon (TOC); (c) C/N ratio; (d) pollen concentration; (e–h) grain size distribution and mean grain size; (i) quantitative reconstruction of mean temperature of the warmest month (Mt_{wa}). The dark purple curve indicates the reconstruction based on the pollen assemblages including the arboreal pollen and the light purple curve represents the reconstruction based on the pollen assemblages removing the arboreal pollen (before 7.4 ka only); (j) the quantitative reconstructions of mean annual precipitation (P_{ann}). The dark blue curve is the reconstruction based on the pollen assemblages including the arboreal pollen, and the light blue curve is the reconstruction based on the pollen assemblages without the arboreal pollen (before 7.4 ka only). The grey shading denotes the different pollen zones of Gahai Lake.

analysed a loess deposit from Ledu on the northeast Tibetan Plateau and also conclude that a grain size of $60\mu\text{m}$ is locally transported by strong winds during cold climatic intervals. The sand fraction ($> 63\mu\text{m}$) is also found in modern river sediments although the percentage is typically low. A single extreme rain event under an arid climate could lead to an abrupt sand fraction increase (Ding et al., 2005; Li et al., 2012; Liu et al., 2016; Ota et al., 2017; Zhou et al., 2018). Therefore, the sand fraction is mainly transported by winds and any peak or abnormal increase of the coarse grain size (especially the sand fraction) is likely related to flood events. In our study, a high proportion of the sand fraction ($> 63\mu\text{m}$) mainly represents aeolian activity intensity.

Particle size variation can reflect changes in water level or precipitation, taking into account the different lake recharge types, hydrological conditions, and lake sizes. There has been debate about how to interpret the grain size index because the coarse particle fraction is positively correlated with precipitation and water level in small lakes dominated by summer rainfall but not in large lakes (Peng et al., 2005; Chen et al., 2021). Gahai Lake is a small, shallow lake and receives most of its precipitation in summer. The coarse particle fraction reflects a humid climate and high lake level ow-

ing to strong hydrological dynamics (Håkanson and Jansson, 1983; Peng et al., 2005; Liu et al., 2008). The silt fraction ($4\text{--}63\mu\text{m}$) in our study is driven by the medium silt ($16\text{--}32\mu\text{m}$) fraction, while the fine and coarse silt fractions remain almost unchanged during the Holocene, hence the fine, medium, and coarse silts are combined into the total silt fraction ($4\text{--}63\mu\text{m}$) for discussion. In addition, the mean grain size is closely related to the sand fraction and poorly reflects the climatic moisture and lake level. Therefore, we speculate that a high silt fraction ($4\text{--}63\mu\text{m}$) in Gahai Lake reflects an increased lake level, while a high clay fraction ($< 4\mu\text{m}$) content reflects a low level.

5.2 Determination of exogenous pollen grains

According to modern pollen research from the Tibetan Plateau and northern China, *Pinus*, *Picea*, and *Betula* are the dominant pollen taxa in forest samples, and these taxa have a good diffusion capacity with their pollen easily transported for long distances from the source (Lu et al., 2004; Ma et al., 2008). *Ulmus* also has good diffusion and can spread up to 40 km away, and can therefore show up as a regional vegetation component in a pollen assemblage (Xu et al., 2007).

In addition, we analysed the non-woodland topsoil samples within 30 km of Gahai Lake ($n = 22$). Results show that arboreal pollen taxa including *Pinus*, *Picea*, and *Betula* are always present (usually at $< 40\%$) in the pollen samples, indicating that they have good diffusivity and are easily transported to areas beyond the pollen source (Figs. A3; A4). Therefore, the main arboreal pollen taxa in the GAH core including *Pinus*, *Picea*, *Betula*, and *Ulmus* are highly diffusive species which may bias the vegetation reconstruction unless the far distance transport is accounted for.

The main pollen taxa have notable spatial distribution characteristics owing to their ecological environment based on modern pollen research and the modern pollen dataset. Arboreal taxa including *Pinus*, *Picea*, and *Betula* are mainly distributed in a warm and humid environment (Lu et al., 2004). *Ulmus* is a drought-tolerant and light-demanding plant which can survive at precipitation levels lower than 200 mm yr^{-1} (Shen et al., 2005). Previous modern pollen studies reveal that *Chenopodiaceae* and *Ephedra* are commonly found in the desert, indicating a tolerance for dry climatic conditions (Yu et al., 2001; Huang et al., 2018; Qin, 2021) and our modern pollen dataset for the east Tibetan Plateau suggests that xerophilous taxa, such as *Ephedra* and *Chenopodiaceae*, are restricted to areas with P_{ann} lower than 400 mm, and almost absent in samples with high precipitation (Fig. 2). Fossil pollen spectra from the Tibetan Plateau with abundant arboreal pollen taxa together with low pollen concentrations are considered to represent extreme arid conditions and sparse vegetation (Kramer et al., 2010; Ma et al., 2019). Therefore, we argue that the arboreal pollen including *Pinus*, *Picea*, and *Ulmus* has been transported by wind from beyond the watershed, and that the high abundance of drought-tolerant herbaceous taxa (weak dispersal ability) and low pollen concentrations indicate a sparse vegetation cover around the lake between 14.2 and 7.4 ka BP, suggesting an extremely arid climate.

5.3 Evolution of vegetation and climate history since the last deglaciation

Palaeo-vegetation and palaeo-climate are reconstructed based on the fossil pollen, TOC, TN, C/N ratios, and grain size record of Gahai Lake since the last deglaciation.

From 14.2 to 10.8 ka BP, alpine steppe or desert covered the study area with the arboreal pollen derived from the surrounding mountains in the south-east of the basin. Pollen-based past P_{ann} reconstructions are mainly in the range of higher than 418 mm (excluding arboreal taxa from pollen spectra) but less than 610 mm (including arboreal taxa from pollen spectra). Remarkably, however, there is little difference between the reconstructed Mt_{wa} based on excluding arboreal taxa (mean 9.1°C) and including arboreal pollen (mean 9.6°C), thus the climate was probably warm and arid during this period (Fig. 7). Quite low TOC and TN contents, and C/N ratios (< 4) suggest that the organic mat-

ter is mainly derived from aquatic plants and little terrestrial biomass productivity under a dry and cold environment (Fig. 7; Zhu et al., 2015). The maximum clay fraction and a high sand fraction in the lake sediments reflect a low water level and intense aeolian activity (Fig. 7). In summary, Gahai Lake was probably a small and shallow pond during this period, with the surrounding vegetation dominated by alpine steppe or desert.

From 10.8 to 7.4 ka BP, Ranunculaceae and Cyperaceae show a slight increase, and alpine steppe occurs across the region (Fig. 5). The reconstruction suggests that Mt_{wa} (mean: $8.5\text{--}9.0^\circ\text{C}$) slightly decreases compared with the former stage, whereas reconstructed P_{ann} (mean: 468–619 mm) is basically steady but still influenced by the exaggerated contribution of exogenous arboreal pollen (Fig. 7). The TOC and C/N ratios rise during the early Holocene, implying an increase in biological productivity although still mainly from aquatic plants (Fig. 7). The silt fraction significantly increases while the clay fraction decreases sharply with small fluctuations in the sand fraction, indicating a slight rise in the water level and intense aeolian activity during the early Holocene (Fig. 7). Therefore, we infer that the vegetation of Gahai Basin was covered by alpine steppe under dry climatic conditions during the early Holocene.

The pollen spectra are dominated by *Pinus* and *Picea* while drought-tolerant taxa (such as *Chenopodiaceae* and *Ephedra*) have low abundances, indicating a vegetation shift from alpine steppe to montane forest between 7.4 and 3.8 ka BP. In addition, the pollen concentration increases markedly, reflecting a greatly enhanced vegetation and moist climate after 7.4 ka BP (Kramer et al., 2010; Ma et al., 2019). The climate reconstruction shows that P_{ann} (mean: 634 mm) and Mt_{wa} (mean: 9.3°C) reach their peaks, suggesting that Gahai Lake is under a warm and wet climate optimum during this period (Fig. 7). In addition, the silt fraction significantly increases to a peak (mean: 70 %), and TOC, TN, and C/N ratios (> 10) markedly increase suggesting that Gahai Lake was at a high stand with increased terrestrial organic matter input having grown from a small pond since 7.4 ka BP. At the same time, the sand fraction decreases to its nadir (mean: 11.7 %), indicating weakened aeolian activity during this period, which could be related to the increased vegetation cover and moisture (Fig. 7). In summary, as Gahai Lake expanded, the surrounding vegetation became montane forest as seen by a shift in the arboreal pollen from extraregional to within catchment. To support this vegetation, the climate was warm and wet, while aeolian activity was weak during the mid-Holocene (Fig. 7).

Between 3.8 and 2.3 ka BP, the pollen spectra are characterized by a high percentage of Poaceae, *Artemisia*, and Asteraceae (major components of alpine steppe), while arboreal pollen taxa, especially *Pinus* and *Picea*, sharply decrease, indicating a tree-line retreat to a lower elevation and a shift in vegetation type to alpine steppe (Herzschuh et al., 2010; Shen et al., 2021; Fig. 5). Reconstructed P_{ann}

(mean: 547 mm) and Mt_{wa} (mean: 8.3 °C) decrease significantly, suggesting climatic conditions deteriorated (Fig. 7). The TOC, TN, and C/N ratios slightly decrease compared with the previous stage, suggesting that the input of organic matter weakened (Fig. 7). The silt fraction substantially decreases while the sand fraction has an increasing trend, suggesting the lake level decreased and aeolian activity increased (Fig. 7). In brief, the climate tended to be arid with enhanced aeolian activity and deteriorating environmental conditions. Alpine steppe dominated across the study region during this period.

From 2.3 to 0.24 ka BP, the dominant taxa change from alpine steppe (Poaceae, *Artemisia*, and Asteraceae) (Ma et al., 2017; Qin, 2021) to alpine meadow (Cyperaceae) components (Herzschuh, 2007; Herzschuh et al., 2010; Fig. 5), and a decrease in reconstructed P_{ann} (537 mm) and Mt_{wa} (7.3 °C) suggest an arid and cold environment (Fig. 7). The TOC, TN, and C/N ratios are almost unchanged suggesting similar total biogenic productivity to the previous stage (Fig. 7). The silt fraction decreases while the sand fraction increases, indicating a lower lake level and stronger aeolian activity than the former stage. Therefore, in this period, the vegetation turned to alpine meadow under an arid and cold climate, and the lake level dropped while aeolian activity increased.

After 0.24 ka BP (1710 CE), the pollen spectra are dominated by Cyperaceae (maximum, 95 %; Fig. 5), with the percentage of Poaceae decreasing while Ranunculaceae increases. Previous vegetation investigations suggest that overgrazing causes the proportion of Cyperaceae to increase and become the dominant taxon, and thus could be an indicator of human activities (Yuan et al., 2004; Miehe et al., 2014; Lin et al., 2016). In addition, modern pollen research also suggests that pollen assemblages are dominated by Cyperaceae in overgrazed sites of alpine steppe and alpine meadow (Duan et al., 2021). According to earlier topsoil studies, Ranunculaceae and Poaceae are important indicators of grazing activities on the northeast Tibetan Plateau, with pollen percentages changing significantly in the overgrazed sites (Wei et al., 2018; Duan et al., 2021). Hence the vegetation during this period could have been disturbed by human activities. In addition, TOC, TN, and pollen concentrations notably increase, indicating that the terrestrial material input strengthened, possibly as a result of increased surface erosion (silt fraction increases; Fig. 7) due to the destruction of vegetation by grazing and pastoral activities. Reduced precipitation and monsoonal activity are also suggested by the increases in TOC, TN, and pollen concentrations.

5.4 Comparison of the regional climate and vegetation records from the northeast Tibetan Plateau in the early Holocene

Climate and vegetation as revealed by pollen records covering the early Holocene on the northeast Tibetan Plateau are inconsistent, which may be due to the following reasons: lo-

cal factors have a greater effect than regional climate (Chen et al., 2020), the distance of sampling sites from forested areas affects the results of vegetation reconstruction (Sun et al., 2017) and different climatic factors influence the regional vegetation distribution of the eastern Tibetan Plateau (Zhao et al., 2011). Based on the results of TOC, grain size, and reconstructed precipitation based on pollen analysis, we infer that Gahai Lake was surrounded by alpine steppe vegetation under an arid climate, and that the arboreal pollen was mainly transported by wind from the surrounding mountains during the early Holocene (Fig. 8a, b, c). Other records from the northeast Tibetan Plateau support these general features of climate and vegetation during the early Holocene. For example, reconstructions from adjacent areas show that the climate and vegetation of the Zoige Basin and Ximencuo Lake based on the pollen records reached their optimum during the mid-Holocene and had a cooler temperature and lower humidity during the early Holocene (Fig. 8f, g, h, i; Zhou et al., 2010; Zhao et al., 2011; Sun et al., 2017; Herzschuh et al., 2014). Multiproxies (e.g. carbonate content, oxygen and carbon stable isotope compositions of authigenic carbonate) also from Gahai Lake suggest that the climate was arid, becoming warm during the early Holocene and then on the whole moist, during the mid-Holocene (Chen et al., 2007). Cheng et al. (2013) analysed the pollen record of Dalianhai Lake (from 16 ka BP) and conclude that this region had a dry climate and was covered by steppe desert during the early Holocene (Fig. 8d). Multiproxy records from Qinghai Lake including pollen, carbonate, TOC, TN, $\delta^{13}C$ of organic matter, redness records, and lake level reveal that this region had a dry climate and weak East Asian summer monsoon (Fig. 8e; Shen et al., 2005; Ji et al., 2005; Liu et al., 2015; Chen et al., 2016). Similar records are found from Koucha Lake (Fig. 8j, k; P_{ann} and T_{ann} based on the pollen record; Herzschuh et al., 2009), Kuhai Lake (Fig. 8l; P_{ann} based on the pollen record; Wischniewski et al., 2011), the arid region of central Asian (moisture variation based on 11 records integrated during the early Holocene: Fig. 8m; Chen et al., 2008, 2020), and Luanhaizi Lake (Fig. 8o; T_{ann} based on the pollen record; Herzschuh et al., 2005, 2010). The pollen assemblages of Donggi Cona Lake show a high percentage of *Ephedra*, which suggests an arid environment in the early Holocene, although the quantitative reconstruction (Fig. 8n; P_{ann} based on the pollen record) shows this period is the wettest stage in the Holocene (Wang et al., 2014; Huang et al., 2018). Based on the above investigations, we can conclude that the climate was arid on the northeast Tibetan Plateau during the early Holocene.

6 Conclusions

Based on modern pollen investigations for the eastern Tibetan Plateau, arboreal pollen can be determined as exogenous taxa when they appear together with drought-tolerant

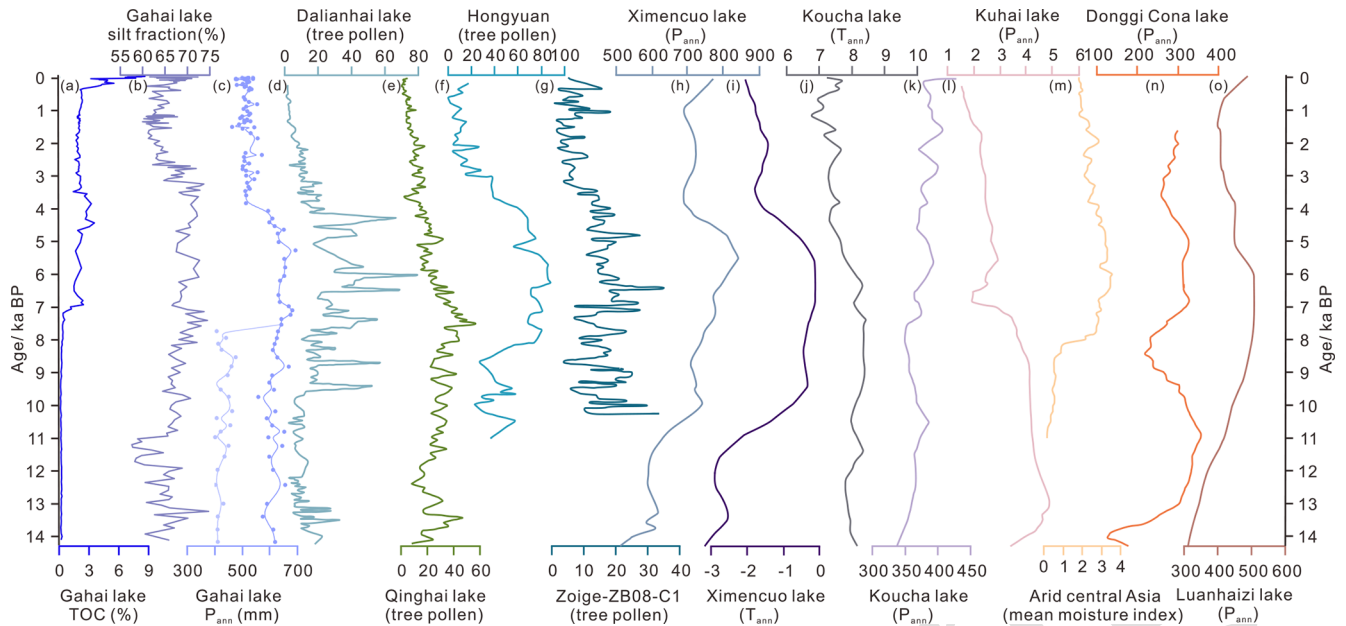


Figure 8. Comparison of the Gahai Lake results with other lake records on the northeast Tibetan Plateau. **(a–c)** Total organic carbon (TOC), silt fraction, and pollen-based precipitation reconstruction of the Gahai Lake record (this paper); **(d)** arboreal pollen percentages of Dalianhai Lake (Cheng et al., 2013); **(e)** arboreal pollen percentages of Qinghai Lake (Shen et al., 2005); **(f)** arboreal pollen percentages of the Hongyuan peatland (Zhou et al., 2010); **(g)** arboreal pollen percentages of the central Zoige basin (Zhao et al., 2011); **(h–i)** P_{ann} and T_{ann} reconstructed from pollen records from Ximencuo Lake (Herzschuh et al., 2014); **(j–k)** T_{ann} and P_{ann} reconstructed from pollen records from Koucha Lake (Herzschuh et al., 2009); **(l)** P_{ann} reconstructed from pollen records from Koucha Lake (Wischnewski et al., 2011); **(m)** synthesized mean moisture index of arid central Asia (Chen et al., 2008); **(n)** P_{ann} reconstructed from pollen records from Donggi Cona Lake (Wang et al., 2014); **(o)** P_{ann} reconstructed from pollen records from Donggi Cona Lake (Herzschuh et al., 2010).

taxa and low pollen concentrations in fossil pollen spectra. The Gahai Basin was covered by alpine steppe or desert under dry climatic conditions during 14.2–7.4 ka BP; montane forest migrated into the basin and the climate reached an optimum between 7.4 and 3.8 ka BP according to the evidence of TN, TOC, C/N, and grain size records; the vegetation reverted to alpine steppe owing to a drying climate from 3.8 to 2.3 ka BP, after which steppe was replaced by alpine meadow as the climate cooled. In addition, the vegetation showed signs of being influenced by human activity during the last 0.24 ka BP.

Appendix A

As noted in the main text, the silt fraction includes fine silt (4–16 μm), medium silt (16–32 μm), and coarse silt (32–63 μm). The proportions of the fine and coarse silt remain almost unchanged during the Holocene, while the medium silt fraction shows the most significant variation. Therefore, in the following sections we use the whole silt fraction (4–63 μm) rather than the different grain sizes of silt fractions.

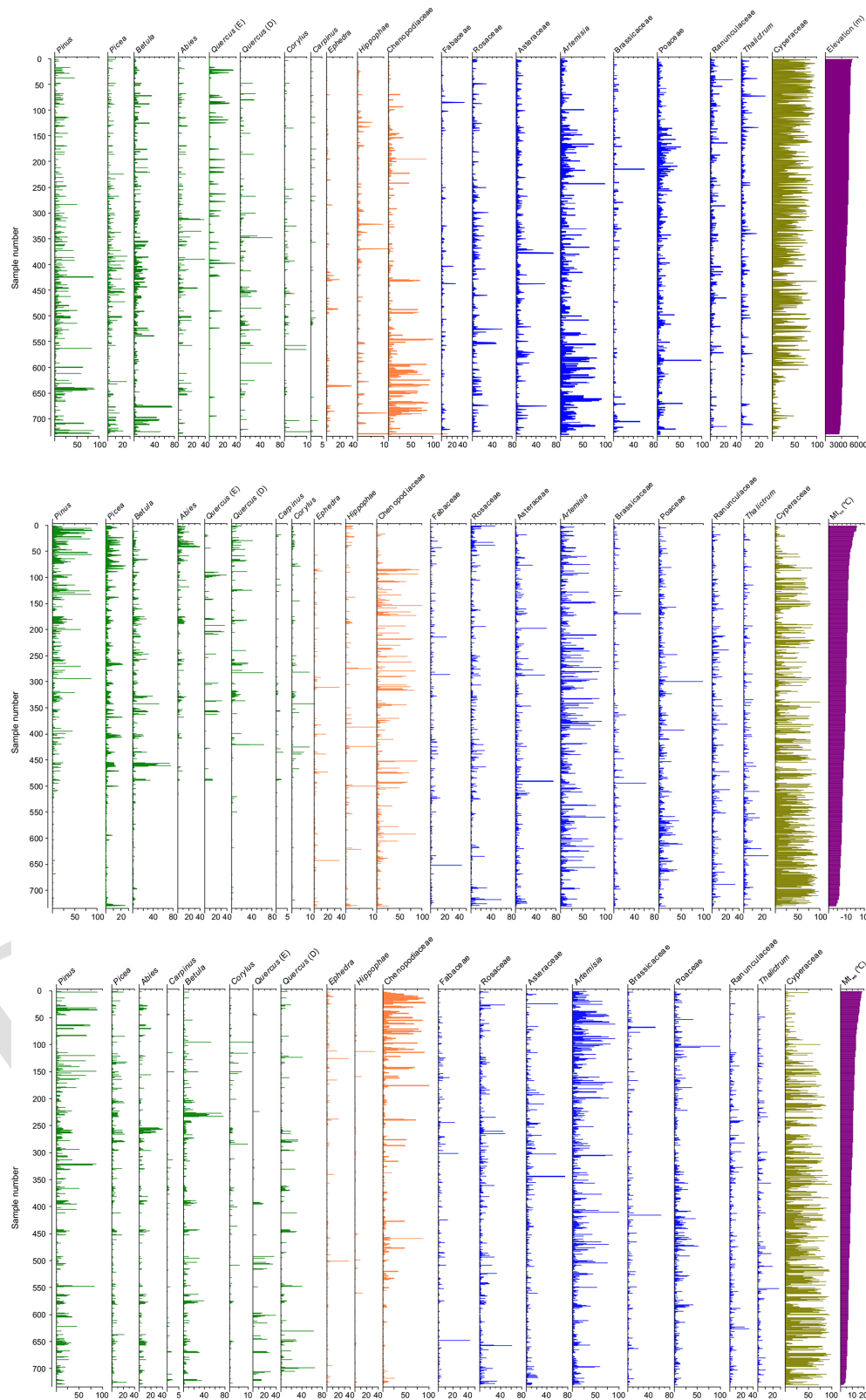


Figure A1. Pollen assemblages of the surface sediment samples arranged along a gradient of climate data from the eastern Tibetan Plateau. Elev: Elevation (m); Mt_{co} : mean temperature of the coldest month (°C); Mt_{wa} : mean temperature of the warmest month (°C).

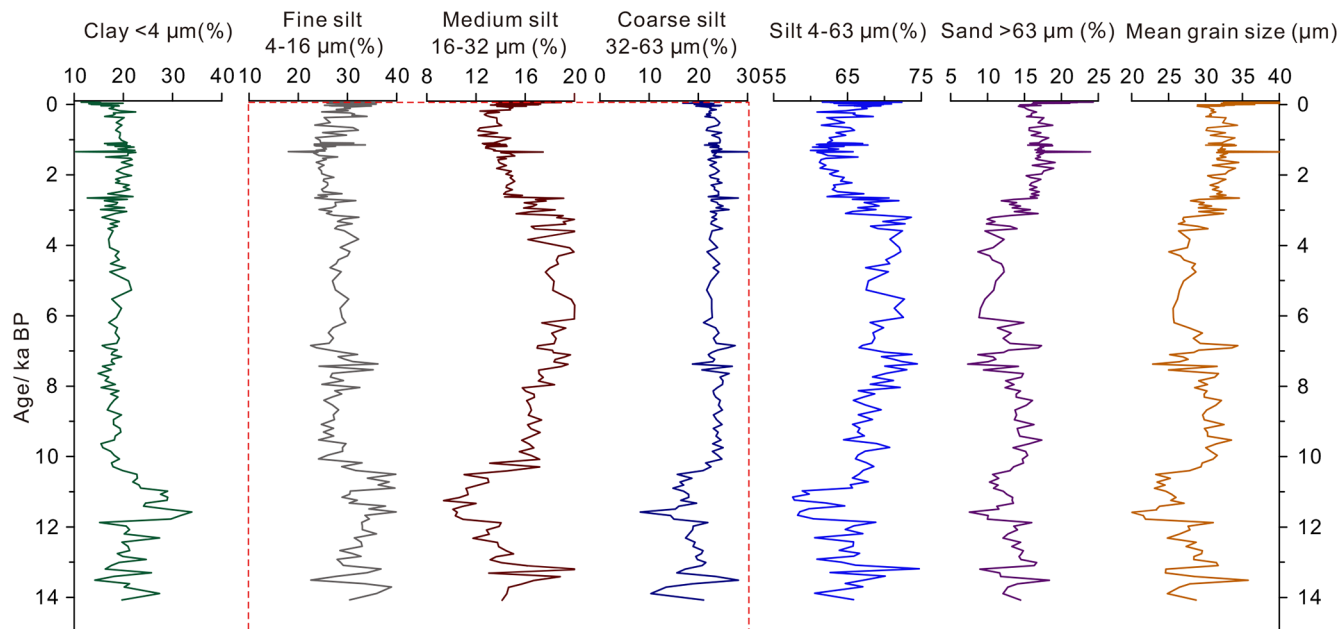


Figure A2. The percentage of different grain size components and mean grain size derived from Gahai Lake since 14.2 ka BP.

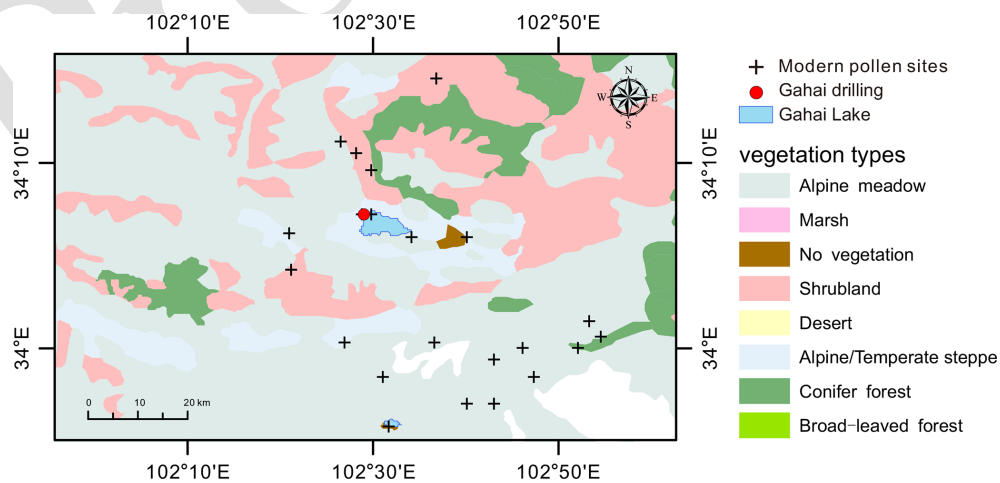


Figure A3. Location of the modern pollen samples ($n = 22$) in the vicinity of Gahai Lake.

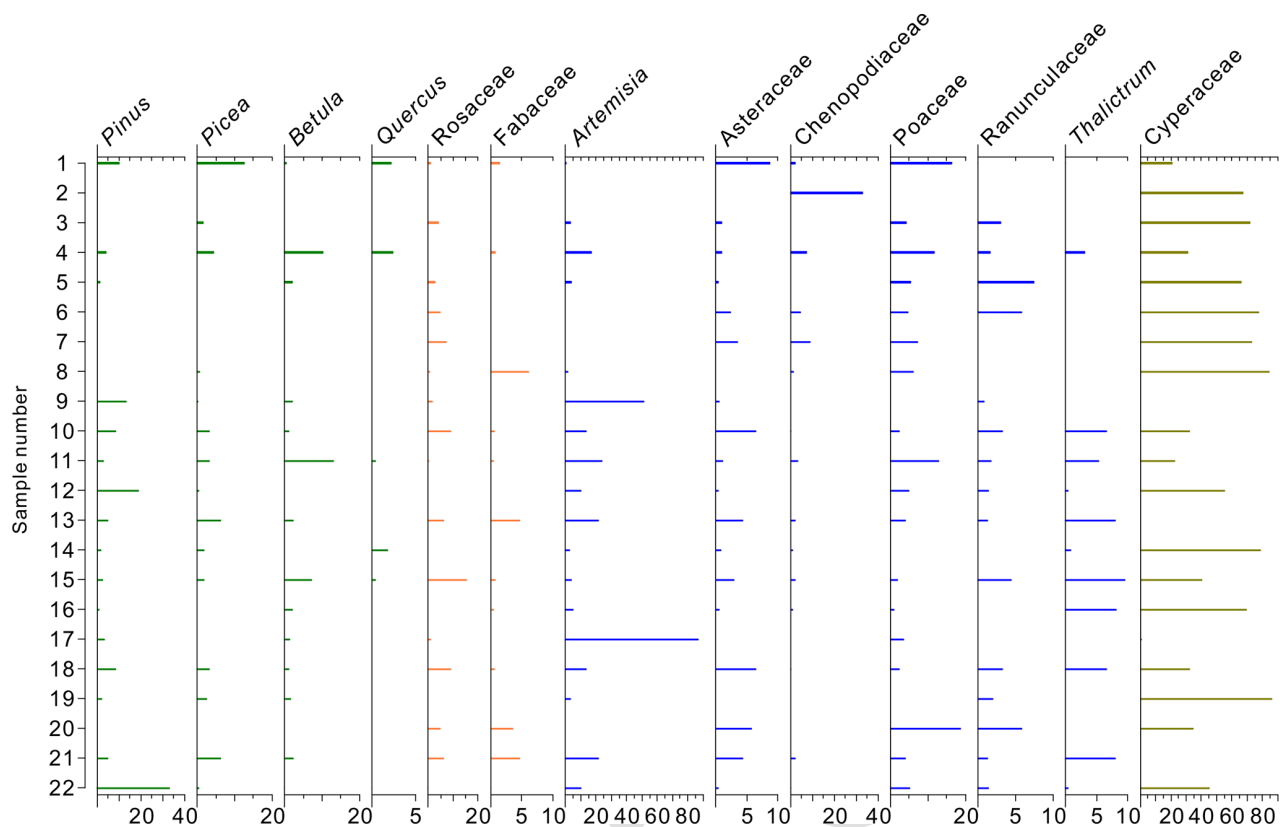



Figure A4. Pollen diagram of the modern pollen samples ($n = 22$) in the vicinity of the Gahai Lake.

Data availability. The data used in this study can be obtained from the corresponding author Xianyong Cao (xcao@itpcas.ac.cn).

Acknowledgements. We would like to thank Cathy Jenks for her help with language editing.

Supplement. The supplement related to this article is available online at: <https://doi.org/10.5194/cp-18-1-2022-supplement>.

Financial support.  This study was supported by the Basic Science Center for Tibetan Plateau Earth System (BSCTPES, NSFC project no. 41988101), the National Natural Science Foundation of China (grant no. 41877459) and the CAS Pioneer Hundred Talents Program (Xianyong Cao).

Author contributions. NW extracted and identified pollen samples, analysed pollen data and wrote the manuscript. LL, XH, and YZ participated in sample collecting and data analysis. HW contributed to the detailed comments. XC designed this study and led the interpretation. All authors commented on and improved the manuscript.

Review statement. This paper was edited by Claudio Latorre and reviewed by two anonymous referees.

Competing interests. The contact author has declared that none of the authors has any competing interests.

Disclaimer. Publisher's note: Copernicus Publications remains neutral with regard to jurisdictional claims in published maps and institutional affiliations.

References

- An, Z., Colman, S. M., Zhou, W., Li, X., Brown, E. T., Jull, A. J. T., Cai, Y., Huang, Y., Lu, X., Chang, H., Song, Y., Sun, Y., Xu, H., Liu, W., Jin, Z., Liu, X., Cheng, P., Liu, Y., Ai, L., Li, X., Liu, X., Yan, L., Shi, Z., Wang, X., Wu, F., Qiang, X., Dong, J., Lu, F., and Xu, X.: Interplay between the westerlies and Asian monsoon recorded in Lake Qinghai sediments since 32 ka, *Scientific Reports*, 2, 619, <https://doi.org/10.1038/srep00619>, 2012.
- Andersen, K. K., Azuma, N., Barnola, J. M., Bigler, M., Biscaye, P., Caillon, N., Chappellaz, J., Clausen, H. B., DahlJensen, D., Fis-

- cher, H., Fluckiger, J., Fritzsche, D., Fujii, Y., Goto-Azuma, K., Gronvold, K., Gundestrup, N. S., Hansson, M., Huber, C., Hvidberg, C. S., Johnsen, S. J., Jonsell, U., Jouzel, J., Kipfstuhl, S., Landais, A., Leuenberger, M., Lorrain, R., Masson-Delmotte, V., Miller, H., Motoyama, H., Narita, H., Popp, T., Rasmussen, S. O., Raynaud, D., Rothlisberger, R., Ruth, U., Samyn, D., Schwander, J., Shoji, H., Siggard-Andersen, M. L., Steffensen, J. P., Stocker, T., Sveinbjornsdottir, A. E., Svensson, A., Takata, M., Tison, J. L., Thorsteinsson, T., Watanabe, O., Wilhelms, F., and White, J. W. C.: High-resolution record of Northern Hemisphere climate extending into the last interglacial period, *Nature*, 431, 147–151, <https://doi.org/10.1038/nature02805>, 2004.
- Appleby, P. G.: Chronostratigraphic techniques in recent sediments, in: *Tracking Environmental Change Using Lake Sediments, Volume 1: Basin Analysis, Coring and Chronological Techniques*, edited by: Last, W. M. and Smol, J. P., Kluwer Academic Publishers, Dordrecht, 171–203, ISBN 0-7923-6482-1, 2001.
- Birks, H. J. B.: Contributions of Quaternary botany to modern ecology and biogeography, *Plant Ecol. Divers.*, 12, 189–385, <https://doi.org/10.1080/17550874.2019.1646831>, 2019.
- Blaauw, M. and Christen, J. A.: Flexible paleoclimate age-depth models using an autoregressive gamma process, *Bayesian. Anal.*, 6, 457–474, <https://doi.org/10.1214/ba/1339616472>, 2011.
- Blaauw, M., Christen, J. A., Aquino Lopez, M. A., Esquivel Vazquez, J., Gonzalez V. O. M., Belding, T., Theiler, J., Gough, B., and Karney, C.: rbacon: age-depth modelling using Bayesian statistics, <https://cran.r-project.org/web/packages/rbacon/index.html> (last access: 29 March 2022), 2021.
- Bryson, R. A.: Airstream climatology of Asia, in: *Proceedings of International Symposium on the Qinghai-Xizang Plateau and Mountain Meteorology*, American Meteorological Society, Boston, MA, 604–617, https://doi.org/10.1007/978-1-935704-19-5_36, 1986.
- Cao, X., Herzschuh, U., Telford, R. J., and Ni, J.: A modern pollen-climate dataset from China and Mongolia: Assessing its potential for climate reconstruction, *Rev. Palaeobot. Palyno.*, 211, 87–96, <https://doi.org/10.1016/j.revpalbo.2014.08.007>, 2014.
- Cao, X., Tian, F., Li, K., and Ni, J.: Atlas of pollen and spores for common plants from the east Tibetan Plateau, National Tibetan Plateau Data Center [data set], <https://doi.org/10.11888/Paleoenv.tpd.270735>, 2020.
- Cao, X., Tian, F., Li, K., Ni, J., Yu, X., Liu, L., and Wang, N.: Lake surface sediment pollen dataset for the alpine meadow vegetation type from the eastern Tibetan Plateau and its potential in past climate reconstructions, *Earth Syst. Sci. Data*, 13, 3525–3537, <https://doi.org/10.5194/essd-13-3525-2021>, 2021.
- Chen, F., Yu, Z., Yang, M., Ito, E., Wang, S., Madsen, D. B., Huang, X., Zhao, Y., Sato, T., Birks, H. J. B., Boomer, I., Chen, J., An, C., and Wünnemann, B.: Holocene moisture evolution in arid central Asia and its out-of-phase relationship with Asian monsoon history, *Quaternary Sci. Rev.*, 27, 351–364, <https://doi.org/10.1016/j.quascirev.2007.10.017>, 2008.
- Chen, F., Qiang, M., Zhou, A., Xiao, S., Chen, J., and Sun, D.: A 2000-year dust storm record from Lake Sugan in the dust source area of arid China, *J. Geophys. Res.-Atmos.*, 118, 2149–2160, <https://doi.org/10.1002/jgrd.50140>, 2013.
- Chen, F., Wu, D., Chen, J., Zhou, A., Yu, J., Shen, J., Wang, S., and Huang, X.: Holocene moisture and East Asian summer monsoon evolution in the northeastern Tibetan Plateau recorded by Lake Qinghai and its environs: a review of conflicting proxies, *Quaternary Sci. Rev.*, 154, 111–129, <https://doi.org/10.1016/j.quascirev.2016.10.021>, 2016.
- Chen, F., Zhang, J., Liu, J., Cao, X., Hou, J., Zhou, L., Xu, X., Liu, X., Wang, M., Wu, D., Huang, L., Zeng, T., Zhang, S., Huang, W., Zhang, X., and Yang, K.: Climate change, vegetation history, and landscape responses on the Tibetan Plateau during the Holocene: A comprehensive review, *Quaternary Sci. Rev.*, 243, 106444, <https://doi.org/10.1016/j.quascirev.2020.106444>, 2020.
- Chen, H., Zhu, L., Wang, Y., Ju, J., Ma, Q., and Xu, T.: Paleoclimate changes over the past 13,000 years recorded by Chibuzhang Co sediments in the source region of the Yangtze River, China, *Palaeogeogr. Palaeoclimatol.*, 573, 110433, <https://doi.org/10.1016/j.palaeo.2021.110433>, 2021.
- Chen, Z., Ma, H., Cao, G., Zhang, X., Zhou, D., Yao, Y., Tan, H., and Gao, Z.: Climate-environmental evolution in Gahai Lake area of Qaidam Basin since Late Last Deglacial Period, *Geochimica*, 36, 578–584, 2007 (in Chinese with English abstract).
- Cheng, B., Chen, F., and Zhang, J.: Palaeovegetational and palaeoenvironmental changes since the last deglacial in Gonghe Basin, northeast Tibetan Plateau, *J. Geogr. Sci.*, 23, 136–146, <https://doi.org/10.1007/s11442-013-0999-5>, 2013.
- Chevalier, M., Davis, B. A. S., Heiri, O., Seppä, H., Chase, B. M., Gajewski, K., Lacourse, T., Telford, R. J., Finsinger, W., Guiot, J., Kühl, N., Maezumi, S. Y., Tipton, J. R., Carter, V. A., Brüssel, T., Phelps, L. N., Dawson, A., Zanon, M., Vallé, F., Nolan, C., Mauri, A., de Vernal, A., Izumi, K., Holmström, L., Marsicek, J., Goring, S., Sommer, P. S., Chaput, M., and Kupriyanov, D.: Pollen-based climate reconstruction techniques for late Quaternary studies, *Earth-Sci. Rev.*, 210, 103384, <https://doi.org/10.1016/j.earscirev.2020.103384>, 2020.
- Ding, Z. L., Derbyshire, E., Yang, S. L., Sun, J. M., and Liu, T. S.: Stepwise expansion of desert environment across northern China in the past 3.5 Ma and implications for monsoon evolution, *Earth Planet. Sc. Lett.*, 237, 45–55, <https://doi.org/10.1016/j.epsl.2005.06.036>, 2005.
- Duan, R., Wei, H., Hou, G., Gao, J., Du, Y., and Qin, Z.: Modern Pollen Assemblages in Typical Agro-Pastoral Ecotone in the Eastern Tibetan Plateau and Its Implications for Anthropogenic Activities, *Front. Ecol. Evol.*, 9, 685942, <https://doi.org/10.3389/fevo.2021.685942>, 2021.
- Duan, Y., Zhao, Y., Wu, Y., He, J., Xu, L., Zhang, X., Ma, L., and Qian, R.: δD values of n-alkanes in sediments from Gahai Lake, Gannan, China: implications for sources of organic matter, *J. Paleolimnol.*, 56, 95–107, <https://doi.org/10.1007/s10933-016-9895-1>, 2016.
- Dykoski, C. A., Edwards, R. L., Cheng, H., Yuan, D. X., Cai, Y., Zhang, M., Lin, Y., Qing, J., An, Z., and Revenaugh, J.: A high-resolution, absolute-dated Holocene and deglacial Asian monsoon record from Dongge Cave, China, *Earth Planet. Sc. Lett.*, 233, 71–86, <https://doi.org/10.1016/j.epsl.2005.01.036>, 2005.
- Fægri, K. and Iversen, J.: *Textbook of pollen analysis*, Munksgaard, Copenhagen, 1975.
- Folk, R. L. and Ward, W. C.: Brazos River bar: a study in the significance of grain size parameters, *J. Sediment. Petrol.*, 27, 3–26, <https://doi.org/10.1306/74D70646-2B21-11D7-8648000102C1865D>, 1957.

- Håkanson, L. and Jansson, M.: Principles of Lake Sedimentology, Springer-Verlag, Berlin, ISBN: 978-3-642-69276-5, 978-3-642-69274-1, 1983.
- Herzschuh, U.: Reliability of pollen ratios for environmental reconstructions on the Tibetan Plateau, *J. Biogeogr.*, 34, 1265–1273, <https://doi.org/10.1111/j.1365-2699.2006.01680.x>, 2007.
- Herzschuh, U., Zhang, C., Mischke, S., Herzschuh, R., Mohammadi, F., Mingram, B., Kürschner, H., and Riedel, F.: A late Quaternary lake record from the Qilian Mountains (NW China), evolution of the primary production and the water depth reconstructed from macrofossil, pollen, biomarker and isotope data, *Global Planet. Change*, 46, 361–379, <https://doi.org/10.1016/j.gloplacha.2004.09.024>, 2005.
- Herzschuh, U., Kürschner, H., and Mischke, S.: Temperature variability and vertical vegetation belt shifts during the last ~50,000 yr in the Qilian Mountains (NE margin of the Tibetan Plateau, China), *Quaternary Res.*, 66, 133–146, <https://doi.org/10.1016/j.yqres.2006.03.001>, 2006.
- Herzschuh, U., Kramer, A., Mischke, S., and Zhang, C.: Quantitative climate and vegetation trends since the late glacial on the northeastern Tibetan Plateau deduced from Koucha Lake pollen spectra, *Quaternary Res.*, 71, 162–171, <https://doi.org/10.1016/j.yqres.2008.09.003>, 2009.
- Herzschuh, U., Birks, H. J. B., Mischke, S., Zhang, C., and Böhner, J.: A modern pollen-climate calibration set based on lake sediments from the Tibetan Plateau and its application to a Late Quaternary pollen record from the Qilian Mountains, *J. Biogeogr.*, 37, 752–766, <https://doi.org/10.1111/j.1365-2699.2009.02245.x>, 2010.
- Herzschuh, U., Borkowski, J., Schewe, J., Mischke, S., and Tian, F.: Moisture advection feedback supports strong early-to-mid Holocene monsoon climate on the eastern Tibetan Plateau as inferred from a pollen-based reconstruction, *Paleogeogr. Paleoclim.*, 402, 44–54, <https://doi.org/10.1016/j.palaeo.2014.02.022>, 2014.
- Hill, M. O. and Gauch, H. G.: Detrended correspondence analysis: an improved ordination technique, *Vegetatio*, 42, 41–58, <https://doi.org/10.1007/BF00048870>, 1980.
- Huang, X., Peng, W., Rudaya, N., Grimm, E. C., Chen, X., Cao, X., Zhang, J., Pan, X., Liu, S., Chen, C., and Chen, F.: Holocene Vegetation and Climate Dynamics in the Altai Mountains and Surrounding Areas, *Geophys. Res. Lett.*, 45, 6628–6636, <https://doi.org/10.1029/2018GL078028>, 2018.
- Ji, J., Shen, J., Balsam, W., Chen, J., Liu, L., and Liu, X.: Asian monsoon oscillations in the northeastern Qinghai–Tibet Plateau since the late glacial as interpreted from visible reflectance of Qinghai Lake sediments, *Earth Planet. Sc. Lett.*, 233, 61–70, <https://doi.org/10.1016/j.epsl.2005.02.025>, 2005.
- Juggins, S.: rioja: Analysis of Quaternary Science Data, version 0.9-26, <https://CRAN.R-project.org/package=rioja>, last access: 28 October 2020.
- Kasper, T., Haberzettl, T., Wang, J., Daut, G., Doberschütz, S., Zhu, L., and Mäusbacher, R.: Hydrological variations on the Central Tibetan Plateau since the LGM and their teleconnections to inter-regional and hemispheric climate variations, *J. Quaternary Sci.*, 30, 70–78, <https://doi.org/10.1002/jqs.2759>, 2015.
- Kramer, A., Herzschuh, U., Mischke, S., and Zhang, C.: Late Glacial vegetation and climate oscillations on the south-eastern Tibetan Plateau inferred from the Lake Naleng pollen profile, *Quaternary Res.*, 73, 324–335, <https://doi.org/10.1016/j.yqres.2009.12.003>, 2010.
- Li, Y., Yu, G., Shen, H., Hu, S., Yao, S., and Yin, G.: Study on lacustrine sediments responding to climatic precipitation and flood discharge in Lake Taihu catchment, China, *Acta Sediment. Sin.*, 30, 1099–1105, 2012 (in Chinese with English abstract).
- Liang, W.: Luqu County Annals, Gansu Culture Press, Lanzhou, 2006 (in Chinese).
- Lin, L., Zhang, D., Cao, G., Ouyang, J., Ke, X., Liu, S., Zhang, F., Li, Y., and Guo, X.: Responses of soil nutrient traits to grazing intensities in alpine Kobresia meadows, *Acta Ecol. Sin.*, 36, 4664–4671, 2016 (in Chinese with English abstract).
- Liu, X., Herzschuh, U., Shen, J., Jiang, Q., and Xiao, X.: Holocene environmental and climatic changes inferred from Wulungu Lake in northern Xinjiang, China, *Quaternary Res.*, 70, 412–425, <https://doi.org/10.1016/j.yqres.2008.06.00>, 2008.
- Liu, X., Lai Z., Madsen, D., and Zeng, F.: Last deglacial and Holocene lake level variations of Qinghai Lake, north-eastern Qinghai–Tibetan Plateau, *J. Quaternary Sci.*, 30, 245–257, <https://doi.org/10.1002/jqs.2777>, 2015.
- Liu, X., Vandenberghe, J., An, Z., Li, Y., Jin, Z., Dong, J., and Sun, Y.: Grain size of Lake Qinghai sediments: implications for riverine input and Holocene monsoon variability, *Paleogeogr. Paleoclim.*, 449, 41–51, <https://doi.org/10.1016/j.palaeo.2016.02.005>, 2016.
- Lu, H., Wang, S., Shen, C., Yang, X., Tong, G., and Liao, G.: Spatial pattern of modern *Abies* and *Picea* pollen in the Qinghai–Xizang Plateau, *Quaternary Sci.*, 24, 39–49, 2004 (in Chinese with English abstract).
- Lu, H., Wu, N., Liu, K.-B., Zhu, L., Yang, X., Yao, T., Wang, L., Li, Q., Liu, X., Shen, C., Li, X., Tong, G., and Jiang, H.: Modern pollen distributions in Qinghai–Tibetan Plateau and the development of transfer functions for reconstructing Holocene environmental changes, *Quaternary Sci. Rev.*, 30, 947–966, <https://doi.org/10.1016/j.quascirev.2011.01.008>, 2011.
- Ma, Q., Zhu, L., Lu, X., Wang, Y., Guo, Y., Wang, J., Ju, J., Peng, P., and Tang, L.: Modern pollen assemblages from surface lake sediments and their environmental implications on the southwestern Tibetan Plateau, *Boreas*, 46, 242–253, <https://doi.org/10.1111/bor.12201>, 2017.
- Ma, Q., Zhu, L., Lü, X., Wang, J., Ju, J., Kasper, T., Daut, G., and Haberzettl, T.: Late glacial and Holocene vegetation and climate variations at Lake Tangra Yumco, central Tibetan Plateau, *Global Planet. Change*, 174, 16–25, <https://doi.org/10.1016/j.gloplacha.2019.01.004>, 2019.
- Ma, Y., Liu, K.-B., Feng, Z., Sang, Y., Wang, W., and Sun, A.: A survey of modern pollen and vegetation along a south–north transect in Mongolia, *J. Biogeogr.*, 35, 1512–1532, <https://doi.org/10.1111/j.1365-2699.2007.01871.x>, 2008.
- Meyers, P. A.: Applications of organic geochemistry to paleolimnological reconstructions: a summary of examples from the Laurentian Great Lakes, *Org. Geochem.*, 34, 261–289, [https://doi.org/10.1016/S0146-6380\(02\)00168-7](https://doi.org/10.1016/S0146-6380(02)00168-7), 2003.
- Meyers, P. A. and Ishiwatari, R.: Lacustrine organic geochemistry – an overview of indicators of organic matter sources and diagenesis in lake sediments, *Org. Geochem.*, 20, 867–900, [https://doi.org/10.1016/0146-6380\(93\)90100-P](https://doi.org/10.1016/0146-6380(93)90100-P), 1993.
- Miehe, G., Miehe, S., Böhner, J., Kaiser, K., Hensen, I., Madsen, D., Liu, J., and Opgenoorth, L.: How old is the hu-

- man footprint in the world's largest alpine ecosystem? A review of multiproxy records from the Tibetan Plateau from the ecologists' viewpoint, *Quaternary Sci. Rev.*, 86, 190–209, <https://doi.org/10.1016/j.quascirev.2013.12.004>, 2014.
- Mykleby, P. M., Snyder, P. K., and Twine, T. E.: Quantifying the trade-off between carbon sequestration and albedo in midlatitude and high-latitude North American forests, *Geophys. Res. Lett.*, 44, 2493–2501, <https://doi.org/10.1002/2016gl071459>, 2017.
- Nychka, D., Furrer, R., Paige, J., and Sain, S.: fields: Tools for spatial data, version 12.3, GitHub [code], <https://github.com/dnynchka/fieldsRPackage>, last access: 17 May 2021.
- Oksanen, J., Blanchet, F. G., Friendly, M., Kindt, R., Legendre, P., McGlinn, D., Minchin, P. R., O'Hara, R. B., Simpson, G. L., Solymos, P., Stevens, M. H. H., Szoecs, E., and Wagner, H.: vegan: Community Ecology Package, version 2.5-4, <https://cran.r-project.org/web/packages/vegan/index.html> (last access: June 2020), 2019.
- Opitz, S., Wünnemann, B., Aichner, B., Dietze, E., Hartmann, K., Herzsuh, U., IJmker, J., Lehmkuhl, F., Li, S., Mischke, S., Plotzki, A., Stauch, G., and Diekmann, B.: Late Glacial and Holocene development of Lake Donggi Cona, north-eastern Tibetan Plateau, inferred from sedimentological analysis, *Palaeogeogr. Palaeoclimatol.*, 337, 159–176, <https://doi.org/10.1016/j.palaeo.2012.04.013>, 2012.
- Ota, Y., Kawahata, H., Sato, T., and Seto, K.: Flooding history of Lake Nakaumi, western Japan, inferred from sediment records spanning the past 700 years, *J. Quaternary Sci.*, 32, 1063–1074, <https://doi.org/10.1002/jqs.2982>, 2017.
- Peng, Y., Xiao, J., Nakamura, T., Liu, B., and Inouchi, Y.: Holocene East Asian monsoonal precipitation pattern revealed by grain-size distribution of core sediments of Daihai Lake in Inner Mongolia of north-central China, *Earth Planet. Sc. Lett.*, 233, 467–479, <https://doi.org/10.1016/j.epsl.2005.02.022>, 2005.
- Prentice, I. C.: Multidimensional scaling as a research tool in Quaternary palynology: a review of theory and methods, *Rev. Palaeobot. Palynol.*, 31, 71–104, [https://doi.org/10.1016/0034-6667\(80\)90023-8](https://doi.org/10.1016/0034-6667(80)90023-8), 1980.
- Qiang, M., Song, L., Chen, F., Li, M., Liu, X., and Wang, Q.: A 16-ka lake-level record inferred from macrofossils in a sediment core from Genggahai Lake, northeastern Qinghai-Tibetan Plateau (China), *J. Paleolimnol.*, 49, 575–590, <https://doi.org/10.1007/s10933-012-9660-z>, 2013.
- Qiang, M., Liu, Y., Jin, Y., Song, L., Huang, X., and Chen, F.: Holocene record of eolian activity from Genggahai Lake, north-eastern Qinghai-Tibetan plateau, China, *Geophys. Res. Lett.*, 41, 589–595, <https://doi.org/10.1002/2013GL058806>, 2014.
- Qin, F.: Modern pollen assemblages of the surface lake sediments from the steppe and desert zones of the Tibetan Plateau, *Sci. China Earth Sci.*, 64, 425–439, <https://doi.org/10.1007/s11430-020-9693-y>, 2021.
- R Core Team: R: A language and environment for statistical computing, R Foundation for Statistical Computing, Vienna, <https://www.r-project.org/> (last access: 23 June 2022), 2021.
- Reimer, P. J., Austin, W. E. N., Bard, E., Bayliss, A., Blackwell, P. G., Bronk Ramsey, C., Butzin, M., Cheng, H., Edwards, R. L., Friedrich, M., Grootes, P. M., Guilderson, T. P., Hajdas, I., Heaton, T. J., Hogg, A. G., Hughen, K. A., Kromer, B., Manning, S. W., Muscheler, R., Palmer, J. G., Pearson, C., Van Der Plicht, J., Reimer, R. W., Richards, D. A., Scott, E. M., Southon, J. R., Turney, C. S. M., Wacker, L., Adolphi, F., Büntgen, U., Capano, M., Fahrni, S. M., Fogtmann-Schulz, A., Friedrich, R., Köhler, P., Kudsk, S., Miyake, F., Olsen, J., Reinig, F., Sakamoto, M., Sookdeo, A., and Talamo, S.: The IntCal20 Northern Hemisphere Radiocarbon Age Calibration Curve (0–55 cal kBP), *Radiocarbon*, 62, 725–757, <https://doi.org/10.1017/RDC.2020.41>, 2020.
- Shen, C., Liu, K., Tang, L., and Overpeck, J.: Modern pollen rain in the Tibetan Plateau, *Front. Earth Sci.*, 9, 732441, <https://doi.org/10.3389/feart.2021.732441>, 2021.
- Shen, J., Liu, X. Q., Wang, S. M., and Matsumoto, R.: Palaeoclimatic changes in the Qinghai Lake area during the last 18,000 years, *Quatern. Int.*, 136, 131–140, <https://doi.org/10.1016/j.quaint.2004.11.014>, 2005.
- Sun, X., Zhao, Y., and Li, Q.: Holocene peatland development and vegetation changes in the Zoige Basin, eastern Tibetan Plateau, *Sci. China Earth Sci.*, 47, 1097–1109, <https://doi.org/10.1007/s11430-017-9086-5>, 2017.
- Tang, L., Mao, L., Shu, J., Li, C., Shen, C., and Zhou, Z.: An Illustrated Handbook of Quaternary Pollen and Spores in China, Science Press, Beijing, 1–621, ISBN: 978-7-03-050568-2, 2017.
- ter Braak, C. J. F. and Prentice, I. C.: A theory of gradient analysis, *Adv. Ecol. Res.*, 18, 271–317, [https://doi.org/10.1016/S0065-2504\(08\)60183-X](https://doi.org/10.1016/S0065-2504(08)60183-X), 1988.
- ter Braak, C. J. F. and Verdonschot, P. F. M.: Canonical correspondence analysis and related multivariate methods in aquatic ecology, *Aquat. Sci.*, 57, 255–289, <https://doi.org/10.1007/BF00877430>, 1995.
- Wang, F., Qian, N., Zhang, Y., and Yang, H.: Pollen Flora of China, Science Press, Beijing, 1–461, 1995 (in Chinese).
- Wang, H., Hu, Y., Zhang, X., Lv, F., Ma, X., W, D., Chen, F., Zhou, A., Hou, J., and Chen, J.: A 17 ka multi-proxy paleoclimatic record on the northeastern Tibetan Plateau: implications for the northernmost boundary of the Asian summer monsoon during the Holocene, *Int. J. Climatol.*, 42, 191–201, <https://doi.org/10.1002/joc.7239>, 2021.
- Wang, N., Liu, L., Zhang, Y., and Cao, X.: A modern pollen data set for the forest–meadow–steppe ecotone from the Tibetan Plateau and its potential use in past vegetation reconstruction, *Boreas*, <https://doi.org/10.1111/bor.12589>, 2022.
- Wang, X., Yi, S., Lu, H., Vandenberghe, J., and Han, Z.: Aeolian process and climatic changes in loess recorded from the NTP: response to global temperature forcing since 30 ka, *Paleoceanography*, 30, 612–620, <https://doi.org/10.1002/2014PA002731>, 2015.
- Wang, Y., Herzsuh, U., Shumilovskikh, L. S., Mischke, S., Birks, H. J. B., Wischniewski, J., Böhner, J., Schlütz, F., Lehmkuhl, F., Diekmann, B., Wünnemann, B., and Zhang, C.: Quantitative reconstruction of precipitation changes on the NE Tibetan Plateau since the Last Glacial Maximum – extending the concept of pollen source area to pollen-based climate reconstructions from large lakes, *Clim. Past*, 10, 21–39, <https://doi.org/10.5194/cp-10-21-2014>, 2014.
- Wang, Y. J., Cheng, H., Edwards, R. L., An, Z. S., Wu, J. Y., Shen, C.-C., and Dorale, J. A.: A high-resolution absolute-dated Late Pleistocene monsoon record from Hulu Cave, China, *Science*, 294, 2345–2348, <https://doi.org/10.1126/science.1064618>, 2001.
- Wei, H., Yuan, Q., Xu, Q., Qin, Z., Wang, L., Fan, Q., and Shan, F.: Assessing the impact of human activities on surface pollen assemblages in Qinghai Lake Basin, China, *J. Quaternary Sci.*, 33, 702–712, <https://doi.org/10.1002/jqs.3046>, 2018.

- Wischniewski, J., Mischke, S., Wang, Y., and Herzschuh, U.: Reconstructing climate variability on the northeastern Tibetan Plateau since the last Lateglacial – a multi proxy, dual-site approach comparing terrestrial and aquatic signals, *Quaternary Sci. Rev.*, 30, 82–97, <https://doi.org/10.1016/j.quascirev.2010.10.001>, 2011.
- Xiao, J., Fan, J., Zhou, L., Zhai, D., Wen, R., and Qin, X.: A model for linking grain-size component to lake level status of a modern clastic lake, *J. Asian Earth Sci.*, 69, 149–158, <https://doi.org/10.1016/j.jseaes.2012.07.003>, 2013.
- Xu, D., Lu, H., Wu, N., Liu, Z., Li, T., Shen, C., and Wang, L.: Asynchronous marine-terrestrial signals of the last deglacial warming in East Asia associated with low- and high-latitude climate changes, *P. Natl. Acad. Sci. USA.*, 110, 9657–9662, <https://doi.org/10.1073/pnas.1300025110>, 2013.
- Xu, Q., Li, Y., Yang, X., and Zheng, Z.: Quantitative relationship between pollen and vegetation in northern China, *Sci. China Ser. D*, 50, 582–599, <https://doi.org/10.1007/s11430-007-2044-y>, 2007.
- Yan, D. and Wünnemann, B.: Late Quaternary water depth changes in Hala Lake, northeastern Tibetan Plateau, derived from ostracod assemblages and sediment properties in multiple sediment records, *Quaternary Sci. Rev.*, 95, 95–114, <https://doi.org/10.1016/j.quascirev.2014.04.030>, 2014.
- Yu, G., Tang, L., Yang, X., Ke, X., and Harrison, S. P.: Modern Pollen Samples from Alpine Vegetation on the Tibetan Plateau, *Global Ecol. Biogeogr.*, 10, 503–519, <https://doi.org/10.1046/j.1466-822x.2001.00258.x>, 2001.
- Yuan, J., Jiang, X., Huang, W., and Wang, G.: Effects of grazing intensity and grazing season on plant species diversity in alpine meadow, *Acta Pratac. Sin.*, 13, 16–21, 2004 (in Chinese with English abstract).
- Zhao, Y., Yu, Z., and Zhao, W.: Holocene vegetation and climate histories in the eastern Tibetan Plateau: controls by insolation-driven temperature or monsoon-derived precipitation changes?, *Quaternary Sci. Rev.*, 30, 1173–1184, <https://doi.org/10.1016/j.quascirev.2011.02.006>, 2011.
- Zhao, Y., Liu, Y., Guo, Z., Fang, K., Li, Q., and Cao, X.: Abrupt vegetation shifts caused by gradual climate changes in central Asia during the Holocene, *Science China Earth Sciences*, 60, 1317–1327, <https://doi.org/10.1007/s11430-017-9047-7>, 2017.
- Zhou, J., Wu, J., and Zeng, H.: Extreme flood events over the past 300 years inferred from lake sedimentary grain sizes in the Altay Mountains, northwestern China, *Chinese Geogr. Sci.*, 28, 773–783, <https://doi.org/10.1007/s11769-018-0968-0>, 2018.
- Zhou, W., Yu, S., Burr, G. S., Kukla, G. J., Jull, A. J. T., Xian, F., Xiao, J., Colman, S. M., Yu, H., Liu, H., Liu, Z., and Kong, X.: Postglacial changes in the Asian summer monsoon system: A pollen record from the eastern margin of the Tibetan Plateau, *Boreas*, 39, 528–539, <https://doi.org/10.1111/j.1502-3885.2010.00150.x>, 2010.
- Zhu, L., Lü, X., Wang, J., Peng, P., Kasper, T., Daut, G., Haberzettl, T., Frenzel, P., Li, Q., Yang, R., Schwalb, A., and Mäusbacher, R.: Climate change on the Tibetan Plateau in response to shifting atmospheric circulation since the LGM, *Scientific Reports*, 5, 13318, <https://doi.org/10.1038/srep13318>, 2015.

Remarks from the language copy-editor

CE1 Please confirm the slight changes in this section.